\$50 CALLED

Contents lists available at ScienceDirect

Probabilistic Engineering Mechanics

journal homepage: www.elsevier.com/locate/probengmech



Finite dimensional models for extremes of Gaussian and non-Gaussian processes



Hui Xu^{a,*}, Mircea D. Grigoriu^{a,b}

- ^a Center for Applied Mathematics, Cornell University, Ithaca, NY, USA
- ^b Department of Civil and Environmental Engineering, Cornell University, Ithaca, NY, USA

ARTICLE INFO

MSC:

60 62

Keywords:

Extremes

Weak convergence

Almost sure convergence

Finite dimensional model

Karhunen-Loève (KL) representation

ABSTRACT

Numerical solutions of stochastic problems involving random processes X(t), which constitutes infinite families of random variables, require to represent these processes by finite dimensional (FD) models $X_d(t)$, i.e., deterministic functions of time depending on finite numbers d of random variables. Most available FD models match the mean, correlation, and other global properties of X(t). They provide useful information to a broad range of problems, but cannot be used to estimate extremes or other sample properties of X(t). We develop FD models $X_d(t)$ for processes X(t) with continuous samples and establish conditions under which these models converge weakly to X(t) in the space of continuous functions as $d \to \infty$. These theoretical results are illustrated by numerical examples which show that, under the conditions established in this study, samples and extremes of X(t) can be approximated by samples and extremes of $X_d(t)$ and that the discrepancy between samples and extremes of these processes decreases with d.

1. Introduction

Most probabilistic models match only some properties of target processes, e.g., current models for wind pressure time series recorded in wind tunnels match the mean and correlation functions [1–4] or the marginal distributions, in addition to and mean and correlation functions, [5–10]. There are no models which match sample properties of target processes, although sample properties are critical for estimating extremes of random processes and related properties [11].

There are at least three reasons for constructing models which capture sample properties, rather than just mean, correlations, and other low order statistics. First, a random process is defined completely by its samples. Mean, variances, correlations, polyspectra and other low order statistics are insufficient to characterize completely random processes, generate samples and estimate extremes of these processes.

Second, processes with the same mean and correlation functions can have very different sample properties and extremes. For example, the processes $X_B(t)$ and $X_C(t)$ defined by $dX(t) = -\rho X(t) dt + \sqrt{2\rho} dY(t)$ with Y(t) denoting the standard Brownian motion process B(t) and a compound Poisson process C(t) have the same mean and correlation functions under proper tuning of the compound Poisson process C(t). Yet, $X_B(t)$ has continuous samples while the samples of $X_C(t)$ exhibit jumps at random times. Also, the extremes $\sup_{t \in [0,\tau]} |X_C(t)|$ and $\sup_{t \in [0,\tau]} |X_B(t)|$ of these processes differ significantly, as illustrated by the histograms of Fig. 1 which are based on 50,000 independent samples of $X_B(t)$ and $X_C(t)$. Note that the two histograms have different

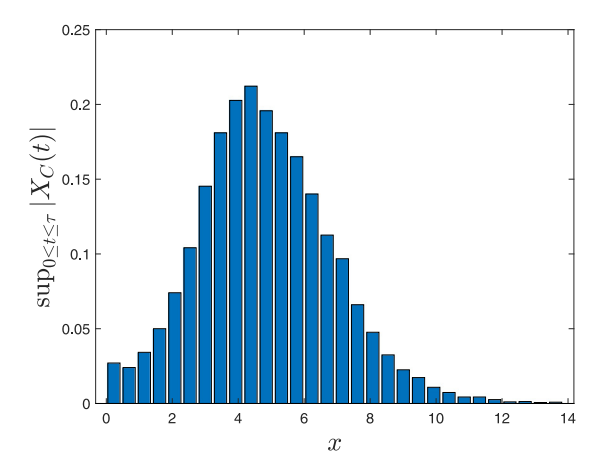
scales and that $\sup_{t\in[0,\tau]}|X_C(t)|$ and $\sup_{t\in[0,\tau]}|X_B(t)|$ are in the ranges [0,14] and [1.5,5.0].

Third, simplified representations of non-Gaussian processes based on heuristic assumptions may not work for extremes. For example, Let $X(t) = G(t)^3$, where $G(t) = A\cos(vt) + B\sin(vt)$, $t \in [0,\tau]$, A,B are independent standard Gaussian variables and $v = 2\pi/\tau$. Hence, $X(t) = \sum_{k=1}^d Z_k \, \varphi_k(t)$, d = 4, where $\{Z_k\}$ are uncorrelated but dependent non-Gaussian variables. The solid line in Fig. 2 is an estimate of the probability $P(\sup_{t \in [0,\tau]} |X(t)| > x)$. The dotted line is an estimate of this probability under a common assumption in applications [12] that the random coefficients $\{Z_k\}$ have the correct distributions but are independent. The plots show that the extremes of X(t) are underestimated under this heuristic assumption in agreement with considerations in [13].

Our objective is to develop finite dimensional (FD) models $\{X_d(t)\}$, d=1,2,..., for real-valued random processes X(t), $t\in[0,\tau]$, with continuous samples, i.e., deterministic functions of time which depend on d random variables, whose samples match in some sense the samples of the target process X(t). The stochastic dimension of $X_d(t)$ is finite and equal to $d<\infty$. In contrast, the stochastic dimension of X(t) is infinity since it consists of an uncountable family of random variables indexed by $t\in[0,\tau]$. It is shown that it is possible to construct FD models such that the discrepancy $\sup_{t\in[0,\tau]}|X(t)-X_d(t)|$ can be made as small as desired by increasing d. Specifically, we show that under some conditions $\sup_{t\in[0,\tau]}|X(t)-X_d(t)|\to 0$ as $d\to\infty$ weakly and/or

E-mail addresses: hx223@cornell.edu (H. Xu), mdg12@cornell.edu (M.D. Grigoriu).

Corresponding author.



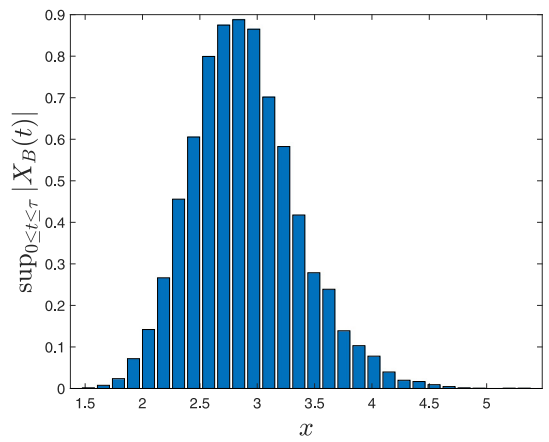


Fig. 1. Histograms of $\sup_{t \in [0,\tau]} |X_C(t)|$ and $\sup_{t \in [0,\tau]} |X_B(t)|$ (left and right panels) for responses $X_C(t)$ and $X_B(t)$ with the same mean and correlation functions, where $\tau = 50$, and $\rho = 1$.

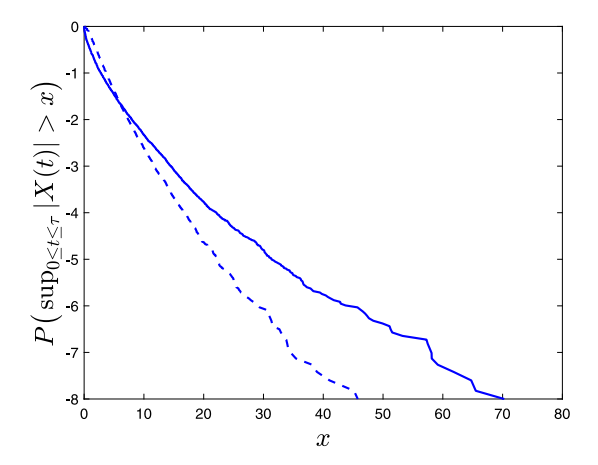


Fig. 2. Estimate of $P\left(\sup_{t\in[0,\tau]}|X(t)|>x\right)$ and approximation under the assumption that $\{Z_k\}$ are independent (solid and dotted lines).

a.s., which means that samples of $X_d(t)$ can be used as substitutes for samples of X(t) for sufficiently large d so that extremes of X(t) can be approximated by those of $X_d(t)$.

The paper is organized as follows. We define finite dimensional models in Section 2 and give their properties. Conditions under which $X_d(t)$ converges weakly to arbitrary processes X(t) in $C[0,\tau]$ are established in Section 3, which contains our main result. The special cases of Gaussian and translation processes X(t) are also discussed. Numerical illustrations of our theoretical results are in Section 4. Section 5 summarizes our findings and the Appendix gives computational details for one of the numerical illustrations.

2. Finite dimensional (FD) models

Consider a real-valued process $\{X(t), t \in [0, \tau]\}$, $0 < \tau < \infty$, defined on a probability space (Ω, \mathcal{F}, P) with mean $\mu(t) = E[X(t)] = 0$ and correlation function c(s,t) = E[X(s) X(t)]. The assumption $\mu(t) = 0$ is not restrictive since, if $\mu(t) \neq 0$, the deterministic function $\mu(t)$ can be added to the samples of X(t). It is assumed that the correlation function of X(t) is continuous, so that it is square integrable on $K = [0,\tau]^2$, i.e., $\int_K c(s,t)^2 ds dt < \infty$. Under this assumption, $A\varphi(t) = \int_K c(s,t) \varphi(s) ds$ is a compact, self-adjoint operator on $L_2(K)$ so that its eigenvalues $\{\lambda_k\}$, $k=1,2,\ldots$, are non-negative and its eigenfunctions $\{\varphi_k(t)\}$, $k=1,2,\ldots$ are orthonormal, i.e., $\langle \varphi_k, \varphi_l \rangle = \int_0^\tau \varphi_k(t) \varphi_l(t) dt = \delta_{kl}$. According to Mercer's theorem [14] (Section 6.2) or [15], the series

 $c(s,t) = \sum_{k=1}^{\infty} \lambda_k \varphi_k(s) \varphi_k(t)$ converges absolutely and uniformly in K. Also, X(t) admits the Karhunen–Loève (KL) representation

$$X_{\mathrm{KL}}(t) = \sum_{k=1}^{\infty} Y_k \, \varphi_k(t),\tag{2.1}$$

where $\{Y_k\}$ are uncorrelated random variables with $E[Y_k]=0$ and $E[Y_k\,Y_l]=\lambda_k\delta_{kl}$. The series in (2.1) converges in mean square (m.s.) for any $t\in[0,\tau]$. This follows from the observation that the FD models

$$X_{\text{KL,d}}(t) = \sum_{k=1}^{d} Y_k \, \varphi_k(t), \quad d = 1, 2, \dots,$$
 (2.2)

which are truncated versions of $X_{\mathrm{KL}}(t)$, are such that $E\left[\left(X_{KL,n}(t)-X_{KL,m}(t)\right)^2\right]=\sum_{k=m+1}^n\lambda_k\varphi_k(t)^2\to 0$, as $m,n\to\infty$, by Mercer's theorem. This shows that $X_{KL,d}(t)$ is Cauchy in $L^2[0,\tau]$ and that the series representation of $X_{KL}(t)$ is m.s. convergent [14] (Theorem 6.2.1). Accordingly, $X_{\mathrm{KL}}(t)$ and X(t) have the same mean and correlation functions. It can also be shown that $E\left[\left(X_{KL}(s)-X_{KL}(t)\right)^2\right]\to 0$ as $s\to t$, $s,t\in[0,\tau]$.

The process $X_{\mathrm{KL},\mathrm{d}}(t)$ in (2.2) is partially specified by its mean and correlation functions which are those of the target process X(t), unless X(t) is Gaussian in which case $\{Y_k\}$ are independent Gaussian variables so that $X_{\mathrm{KL},\mathrm{d}}(t)$ is a Gaussian process with the first two moments of X(t). If X(t) is not Gaussian, the random variables $\{Y_k\}$ are uncorrelated but dependent non-Gaussian variables. Since the joint distribution of $\{Y_k\}$ is unknown, it is not possible to generate samples of, e.g., truncated versions $X_{KL,\mathrm{d}}(t)$ of $X_{\mathrm{KL}}(t)$.

We construct an alternative sequence $\{X_d(t)\}$ of finite dimensional (FD) processes which is closely related to that in (2.2) in the sense that it shares the same basis functions, i.e., the eigenfunctions $\{\varphi_k\}$ of the correlation function of X(t). It has the expression

$$X_d(t) = \sum_{k=1}^{d} Z_k \, \varphi_k(t), \quad d = 1, 2, \dots,$$
 (2.3)

where the random coefficients $\{Z_k\}$ are defined sample-by-sample from samples of X(t) by projection, i.e.,

$$Z_k(\omega) = \int_0^\tau X(t, \omega) \varphi_k(t) dt, \ k \ge 1, \quad \omega \in \Omega,$$
 (2.4)

where $X(t,\omega)$ denotes a sample of X(t). We note that (1) the processes $\{X_d(t)\}$ are completely defined, (2) samples $X_d(t,\omega)$ and $X(t,\omega)$ of $X_d(t)$ and X(t) are paired by construction and (3) the processes $X_d(t)$ and $X_{\mathrm{KL},d}(t)$ have the same mean and correlation functions. The latter statement follows from the observations that

$$E[Z_k] = E\left[\int_0^\tau X(t)\,\varphi_k(t)\,dt\right] = \int_0^\tau E[X(t)]\,\varphi_k(t)\,dt = 0$$

$$\begin{split} E[Z_k | Z_l] &= E\left[\int_{[0,\tau]^2} X(s) \, X(t) \, \varphi_k(s) \, \varphi_l(t) \, ds \, dt\right] \\ &= \int_{[0,\tau]^2} E[X(s) \, X(t)] \, \varphi_k(s) \, \varphi_l(t) \, ds \, dt \\ &= \int_0^\tau \left[\int_0^\tau c(s,t) \, \varphi_l(t) \, dt\right] \varphi_k(s) \, ds = \lambda_l \, \int_0^\tau \varphi_l(s) \, \varphi_k(s) \, ds \\ &= \lambda_l \, \delta_{kl}. \end{split}$$

where the change of order of integration holds by Fubini's theorem. It also shows that, like $X_{KL,d}(t)$, $X_d(t)$ converges in m.s. to X(t) as $d \to \infty$.

Consider an arbitrary set of times (t_1, \ldots, t_m) . Since the random vectors $(X_{\text{KL,d}}(t_1), \dots, X_{\text{KL,d}}(t_m))$ and $(X_d(t_1), \dots, X_d(t_m))$ converge in m.s. to $(X(t_1), \dots, X(t_m))$ if their components converge in m.s., then their convergence also hold in probability by Chebyshev's inequality. This implies the convergence of the finite dimensional distributions of $X_d(t)$ to those of X(t) as $d \to \infty$ [16] (Theorem 18.10).

We note that FD processes of the type in (2.3) can be constructed by using other basis functions, e.g., trigonometric polynomials or other sets of orthogonal functions. We use mainly the eigenfunctions of the correlation functions of X(t), since they minimize the mean square error and are delivered by available numerical algorithms.

The subsequent section considers processes X(t) with continuous samples and shows that the sequence of processes $\{X_d(t)\}\$ converges weakly to X(t) in the space of continuous functions $C[0, \tau]$ under some conditions. The processes $\{X_{KL,d}(t)\}\$ do not have this property since their samples are available only for Gaussian target processes X(t)and, if available, cannot be paired with sample of X(t) so that the discrepancy between samples of $\{X_{\mathrm{KL},\mathrm{d}}(t)\}$ and X(t) cannot be assessed.

3. Main results

We follow the approach of Theorems 8.1 and 8.2 or 8.3 in [17] to show that $X_d(t)$ converges weakly to X(t) in $C[0,\tau]$, a convergence which is denoted by $X_d(t) \stackrel{w}{\to} X(t)$. Let $X_d(t), X(t) : (\Omega, \mathcal{F}, P) \to$ $(C[0,\tau],\mathcal{C})$ be real-valued processes with continuous samples, where C denotes the Borel σ -algebra on the space of real-valued continuous functions $C[0, \tau]$. According to Theorem 8.1, the family of processes $\{X_d(t)\}\$ converges weakly to X(t) in $C[0,\tau]$ if (1) the finite dimensional distributions of $X_d(t)$ converge to those of X(t) and (2) the family of processes $\{X_d(t)\}\$ is tight in $C[0,\tau]$. We say that the family $\{X_d(t)\}\$ is tight if for any $\varepsilon > 0$, there exists a compact set $K \subset C[0, \tau]$ such that $P(X_d(t) \in K) > 1 - \varepsilon$ for all d. Theorems 8.2 and 8.3 provide criteria for checking whether a sequence of probability measures is tight, and we use the conditions of these theorems to determine whether the family $\{X_d(t)\}\$ of processes is tight. Since we already have shown the convergence of the finite dimensional distributions of $X_d(t)$ to those of X(t), we only need to show the tightness of the family $\{X_d(t)\}$ of processes to prove that $X_d(t)$ converges weakly to X(t) in $C[0, \tau]$. The following theorem is our main result.

Theorem 3.1. If the finite dimensional distributions of $X_d(t)$ converge to those of X(t), X(t) has continuous samples and continuous correlation function and either (i) or (ii) holds, then

$$\sup_{t \in [0,\tau]} |X_d(t) - X(t)| \stackrel{w}{\to} 0, \ d \to \infty, \tag{3.1}$$

where
$$X_d(t)$$
 is given by (2.3).
 (i) $\sum_{k=1}^{\infty} \sqrt{E[Z_k^2]} L_k(\tau) < \infty$, where $L_k(\delta) = \sup_{|s-t| \le \delta} |\varphi_k(t) - \varphi_k(s)|$, $\delta \in [0, \tau]$.

(ii) There is M > 0 such that $E[\sup_{t \in [0,\tau]} |\dot{X}_d(t)|] \le M$ for all $d \ge 1$ and $\{\varphi_k(t)\}$, $k \ge 1$, are continuously differentiable functions.

Proof. Following Theorem 8.2 in [17], we first show the tightness of the family of random variables $\{X_d(0)\}$. Note that

$$E[X_d(0)^2] = \sum_{k=1}^d \lambda_k \varphi_k(0)^2 \le \sum_{k=1}^\infty \lambda_k \varphi_k(0)^2 = E[X(0)^2] < \infty, \ \forall \ d \ge 1,$$

by Mercer's theorem and $EX(0)^2$ is finite by assumption. Then for any $\varepsilon > 0$ there exists L > 0 such that

$$P(|X_d(0)| > L) \le \frac{1}{L^2} E[X_d(0)^2] \le \frac{1}{L^2} E[X(0)^2] \le \varepsilon, \ \forall d \ge 1$$

by Chebyshev's inequality. Therefore $\{X_d(0)\}$ is tight.

Consider now the second condition of Theorem 8.2, which requires to show that, for given $\varepsilon, \eta > 0$, there exists $\delta_0 > 0$ such that $P(W(\delta_0) \ge$ ε) $\leq \eta$ for $d \geq d_0$, where $W(\delta_0) = \sup_{|s-t| \leq \delta_0} |X_d(t) - X_d(s)|$ denotes the modulus of continuity of $X_d(t)$. We show that the sequence $\{X_d(t)\}$ of processes satisfies this condition provided that (i) or (ii) holds.

Case one (i) holds: for given $\varepsilon > 0$, we have

$$\begin{split} P\bigg(\sup_{|s-t| \leq \delta} |X_d(t) - X_d(s)| \geq \varepsilon \bigg) &\leq P\bigg(\sup_{|s-t| \leq \delta} \bigg| \sum_{k=1}^d Z_k(\varphi_k(t) - \varphi_k(s)) \bigg| \geq \varepsilon \bigg) \\ &\leq P\bigg(\sum_{k=1}^d |Z_k| \sup_{|s-t| \leq \delta} |\varphi_k(t) - \varphi_k(s)| \geq \varepsilon \bigg) \\ &\leq \frac{1}{\varepsilon} \sum_{k=1}^d E|Z_k| \sup_{|s-t| \leq \delta} |\varphi_k(t) - \varphi_k(s)| \\ &= \frac{1}{\varepsilon} \sum_{k=1}^\infty E|Z_k| L_k(\delta). \end{split}$$

Since $L_k(\delta)$ is monotonically increasing, $\sum_{k=1}^{\infty} E|Z_k|L_k(\tau) < \infty$ and each $\varphi_k(t)$ is continuous so that $L_k(\delta)$ is bounded, then by dominated convergence theorem [18] (Theorem 1.34), we know that for any $\varepsilon, \eta >$ 0, there exists δ_0 such that

$$P\bigg(\sup_{|s-t|\leq \delta_0}|X_d(t)-X_d(s)|\geq \varepsilon\bigg)\leq \eta, \ \forall d\geq 1,$$

which implies $X_d(t)$ is tight in $C[0, \tau]$. Since we assume the weak convergence of finite dimensions of $X_d(t)$, we conclude by Theorem 8.1 in [17] that $X_d(t) \stackrel{w}{\to} X(t)$ in the space $C[0, \tau]$ as $d \to \infty$.

Case two (ii) holds: we have for any $k \ge 1$,

$$\begin{split} &P\bigg(\sup_{|s-t|\leq \delta}|X_d(t)-X_d(s)|\geq \varepsilon\bigg)=P\bigg(\sup_{|s-t|\leq \delta}\Big|\sum_{k=1}^d Z_k(\varphi_k(t)-\varphi_k(s))\Big|\geq \varepsilon\bigg)\\ &=\int_{\mathbb{R}^d}P\bigg(\sup_{|s-t|\leq \delta}\Big|\sum_{k=1}^d Z_k(\varphi_k(t)-\varphi_k(s))\Big|\\ &\geq \varepsilon|Z_1=z_1,\ldots,Z_d=z_d\bigg)F(dz_1\cdots dz_d)\\ &=\int_{\mathbb{R}^d}\mathbf{1}\bigg(\sup_{|s-t|\leq \delta}\Big|\sum_{k=1}^d z_k(\varphi_k(t)-\varphi_k(s))\Big|\geq \varepsilon\bigg)F(dz_1\cdots dz_d), \end{split}$$

where F is the joint distribution function of (Z_1, \dots, Z_d) . Let $h_d(t; z_1, \dots, z_d)$ $\ldots, z_d) = \sum_{k=1}^d z_k \varphi_k(t)$ for fixed z_1, \ldots, z_d , since z_1, \ldots, z_d are bounded almost surely, then by mean value theorem there exists ξ between s and t such that

$$h_d(t; z_1, \dots, z_d) - h_d(s; z_1, \dots, z_d) = (t - s)h'_d(\xi; z_1, \dots, z_d),$$

since $\varphi_k(t)$ is assumed to be continuously differentiable, which implies

$$\begin{split} \sup_{|s-t| \leq \delta} \Big| \sum_{k=1}^d z_k (\varphi_k(t) - \varphi_k(s)) \Big| \\ &= \sup_{t \in [s-\delta, s+\delta]} |h_d(t; z_1, \dots, z_d) - h_d(s; z_1, \dots, z_d)| \\ &= \sup_{t \in [s-\delta, s+\delta]} |(t-s)h'_d(\xi; z_1, \dots, z_d)|. \end{split}$$

Note that ξ is between s and t and $t \in [s - \delta, s + \delta]$, then

$$\begin{split} \sup_{|s-t| \leq \delta} \bigg| \sum_{k=1}^d z_k(\varphi_k(t) - \varphi_k(s)) \bigg| &\leq \delta \sup_{t \in [s-\delta, s+\delta]} |h'_d(\xi; z_1, \dots, z_d)| \\ &\leq \delta \sup_{\xi \in [s-\delta, s+\delta]} |h'_d(\xi; z_1, \dots, z_d)|, \end{split}$$

which implies

$$\begin{split} &P\bigg(\sup_{|s-t|\leq \delta}|X_d(t)-X_d(s)|\geq \varepsilon\bigg)\\ &\leq \int_{\mathbb{R}^d}\mathbf{1}\bigg(\delta\sup_{\xi\in[s-\delta,s+\delta]}|h_d'(\xi;z_1,\ldots,z_d)|\geq \varepsilon\bigg)F(dz_1\cdots dz_d)\\ &= P\bigg(\sup_{\xi\in[s-\delta,s+\delta]}|\dot{X}_d(\xi)|\geq \frac{\varepsilon}{\delta}\bigg) \end{split}$$

By Markov inequality and $E[\sup_{t\in[0,\tau]}|\dot{X}_d(t)|]\leq M$ for all $d\geq 1$, take $\delta=\varepsilon\eta/M$, we have

$$P\bigg(\sup_{|s-t|\leq \delta}|X_d(t)-X_d(s)|\geq \varepsilon\bigg)\leq \frac{\delta}{\varepsilon}E\bigg[\sup_{\xi\in [s-\delta,s+\delta]}|\dot{X}_d(\xi)|\bigg]\leq \frac{M\delta}{\varepsilon}=\eta.$$

Hence $X_d(t)$ is tight in $C[0, \tau]$. This property and the convergence of the finite dimensional distributions of $X_d(t)$ to those of X(t) imply

$$\sup_{t \in [0,\tau]} |X_d(t) - X(t)| \xrightarrow{w} 0, \ d \to \infty. \quad \Box$$

In applications, we can use the condition (i) or (ii) depending on properties of X(t). For example, the condition (ii) holds for m.s. differentiable processes, see Theorem 3.2 and Corollary 3.1. Otherwise, we can use the condition (i) as illustrated in Corollaries 3.2 and 3.3.

Remark 3.1. The Brownian motion process B(t), $0 \le t \le 1$, does not satisfy the conditions of the previous theorem. Yet, the family of FD models $\{B_d(t)\}$ of this process constructed as in (2.3) is tight and converges weakly and almost surely to B(t) in the space of continuous functions.

Proof. The sequence $\{B_d(0)\}$ of random variables is tight, since $B_d(0)=B(0)=0$ for any $d\geq 1$. The difference $B_d(s)-B_d(t)=\sum_{k=1}^d Z_k\,\psi_k(s,t)$ is a zero-mean Gaussian random variable with variance $\sum_{k=1}^d \lambda_k\psi_k(s,t)^2$, where $\psi_k(s,t)=\varphi_k(s)-\varphi_k(t)=2^{3/2}\sin((k-1/2)\pi(s-t)/2)\cos((k-1/2)\pi(s+t)/2)$, $k=1,2,\ldots$, and $s,t\in [0,1]$. Then,

$$E[|B_d(s) - B_d(t)|^4] = 3\left(\sum_{k=1}^d \lambda_k \, \psi(s, t)^2\right)^2 \le 3\left(\sum_{k=1}^\infty \lambda_k \, \psi(s, t)^2\right)^2$$
$$= E[|B(s) - B(t)|^4] = 3(s - t)^2$$

by properties of the Gaussian variables and the fact that $\sum_{k=1}^d \lambda_k \, \psi_k(s,t)^2$ increases with d and is bounded. This shows that the second condition of the Theorem 12.3 in [17] is satisfied for $\gamma=4,\ \alpha=2$ and the monotonically increasing and continuous function $h(t)=\sqrt{3}t$, so that B_d converges weakly to B in C[0,1]. This also implies the convergence $B_d \xrightarrow{a.s.} B$ in C[0,1] as $d \to \infty$ by the Itô-Nisio theorem in [19].

It is not surprising that the Brownian motion process B(t) does not satisfy the conditions of our main result although the family $\{B_d(t)\}$ of its FD models converges weakly to B(t) in C[0,1] since the statement of the theorem does not make any assumption on the distribution of the target process X(t). In contrast, the above proof of the remark uses explicitly the fact that B(t) is a Gaussian process with independent increments.

We now develop conditions for the weak convergence of FD models $\{X_d(t)\}$ for Gaussian processes X(t) with smooth samples based on the condition (ii) of Theorem 3.1.

Theorem 3.2. Let G(t) be a zero-mean Gaussian process with continuous samples and continuous correlation function and let $G_d(t)$ defined by (2.3) be a finite dimensional model of G(t). Then

$$\sup_{t \in [0,\tau]} |G_d(t) - G(t)| \stackrel{a.s.}{\to} 0, \ d \to \infty.$$
(3.2)

Proof. Following Theorem 8.3 in [17], we first show that the sequence $\{G_d(0)\}$ of random variables is tight. This follows from the observation that for any $\varepsilon > 0$, there exists L such that

$$\begin{split} P(|G_d(0)| > L) & \leq \frac{1}{L^2} E[G_d(0)^2] = \frac{1}{L^2} E\left[\sum_{k=1}^d Z_k \varphi_k(0)\right]^2 \\ & = \frac{1}{L^2} \sum_{k=1}^d E[Z_k^2] \varphi_k(0)^2 \leq \frac{1}{L^2} \sum_{k=1}^\infty E[Z_k^2] \varphi_k(0)^2 \\ & = \frac{1}{L^2} E[G(0)^2] \leq \varepsilon, \ \forall d \geq 1. \end{split}$$

Then, we show that the sequence of processes $\{G_d(t)\}$ is tight in $C[0,\tau]$ by showing that the second condition of Theorem 8.3 holds. Note that for any fixed $s \in [0,\tau]$ and $\delta > 0$, $[s,s+\delta]$ is a closed interval of \mathbb{R} , so that there exists constant K for $\varepsilon = 1/2$ such that [20] lemma 3.1 or [21]

$$P\left(\sup_{t\in[s,s+\delta]}(G_d(t)-G_d(s))>\lambda\right)\leq Ke^{-(1-\varepsilon)\lambda^2/2\sigma_d^2},\quad \lambda>0.$$

which implies

$$\begin{split} &P\bigg(\sup_{t\in[s,s+\delta]}\left|G_d(t)-G_d(s)\right|>\lambda\bigg)\\ &=P\bigg(\left\{\sup_{t\in[s,s+\delta]}(G_d(t)-G_d(s))>\lambda\right\}\bigcup\bigg\{\sup_{t\in[s,s+\delta]}(G_d(s)-G_d(t))>\lambda\bigg\}\bigg)\\ &\leq P\bigg(\sup_{t\in[s,s+\delta]}(G_d(t)-G_d(s))>\lambda\bigg)+P\bigg(\sup_{t\in[s,s+\delta]}(G_d(s)-G_d(t))>\lambda\bigg)\\ &<2Ke^{-\lambda^2/4\sigma_d^2}. \end{split}$$

where $\sigma_d^2 = \sup_{t \in [s,s+\delta]} \operatorname{Var}[G_d(t) - G_d(s)]$ is finite, since $E[(G_d(t) - G_d(s))^2] \leq E[(G(t) - G(s))^2]$ and $E[(G(t) - G(s))^2] < \infty$ for all $t, s \in [0,\tau]$ by assumption that the correlation function is continuous. Moreover, we can find δ such that $\sup_{t \in [s,s+\delta]} E[(G(t) - G(s))^2]$ is as small as desired. Then for any $\varepsilon, \eta > 0$, there exists δ_0 such that $\sup_{t \in [s,s+\delta_0]} E[(G(t) - G(s))^2] \leq \varepsilon^2/(4\log(2K/\eta))$. Further, for any $d \geq 1$, we have

$$\begin{split} &P\bigg(\sup_{t\in[s,s+\delta_0]}|G_d(t)-G_d(s)|>\varepsilon\bigg)\\ &\leq 2K\exp\bigg\{-\frac{\varepsilon^2}{4\sup_{t\in[s,s+\delta_0]}\mathrm{Var}[G_d(t)-G_d(s)]}\bigg\}\\ &\leq 2K\exp\bigg\{-\frac{\varepsilon^2}{4\sup_{t\in[s,s+\delta_0]}E[(G(t)-G(s))^2]}\bigg\}\leq \eta. \end{split}$$

Therefore the second condition of Theorem 8.3 in [17] holds, which means that $\sup_{t\in[0,\tau]}|G_d(t)-G(t)|\overset{w}{\to}0$, $d\to\infty$. Since $G_d(t)$ is the sum of independent normal random variables for fixed t, i.e., the random variables $Z_k\varphi_k(t)$, then G_d converges a.s to G in $C[0,\tau]$ by Itô-Nisio theorem [19].

We extend the above result to a class of non-Gaussian processes, referred to as translation processes, which are monotonically increasing mappings of Gaussian processes. Let X(t) be a translation process defined by

$$X(t) = F^{-1} \circ \Phi(G(t)), \tag{3.3}$$

where G(t) is a stationary Gaussian process with zero mean and unit variance, Φ denotes the distribution of the standard normal variable and F is the marginal distribution of X(t). The translation processes $\{X(t)\}$ are completely defined by the marginal distribution F and the correlation function of G(t). Translation processes exist if the selected marginal distributions and the correlation functions satisfy some compatibility conditions [22]. Generally, these conditions are mild, since the correlation functions of the translation processes and their Gaussian images are similar. Translation processes match exactly/approximately specified distribution/correlation functions [8,9]. They have been used extensively in applications, e.g., to characterize wind pressure coefficients in Wind Engineering [7,23].

Theorem 3.3. Let X(t) be defined in (3.3) and $X_d(t) = F^{-1} \circ \Phi(G_d(t))$, $t \in [0, \tau]$, where $G_d(t)$ is a finite dimensional model of a Gaussian process G(t), see (2.3). If G(t) satisfies the conditions of Theorem 3.2 and F is continuous and strictly monotonically increasing, then

$$\sup_{t \in [0,\tau]} \left| X_d(t) - X(t) \right| \overset{a.s.}{\to} 0, \ d \to \infty.$$

Proof. Let $U_d(t) = \Phi(G_d(t))$ and $U(t) = \Phi(G(t))$. According to Theorem 3.2 and mean value theorem, we have

$$\sup_{t\in[0,\tau]}|U_d(t)-U(t)|\leq \frac{1}{\sqrt{2\pi}}\sup_{t\in[0,\tau]}|G_d(t)-G(t)|\overset{a.s.}{\to}0,\ d\to\infty.$$

Since F^{-1} is continuous, then F^{-1} is uniformly continuous on [0,1], which leads to $\sup_{t \in [0,r]}$

$$|X_d(t) - X(t)| \stackrel{a.s.}{\to} 0, d \to \infty.$$

As previously stated, there are other FD models in addition to those in (2.3). The following theorem considers FD models $X^{(N)}(t)$ whose samples interpolate linearly between values of X(t) at the times $(0,\Delta t,\ldots,N\,\Delta t)$, where $\Delta t=\tau/N$. The samples of these FD models are continuous functions so that they are elements of $C[0,\tau]$. Under the conditions of the following theorem, the discrepancy between the samples of $X^{(N)}(t)$ and those of $X^{(N)}(t)$ measured by the metric of $C[0,\tau]$ can be made as small as desired by increasing N. Generally, the stochastic dimension N+1 of $X^{(N)}(t)$ is much larger than that of $X_d(t)$ in (2.3) so that they are less useful in applications.

Theorem 3.4. If E[X(t)] = 0, r(s,t) = E[X(t)X(s)] is continuous in t and s and

$$\sup_{|s-t| \le \delta} |X(t) - X(s)| \stackrel{w}{\to} 0, \ \delta \to 0,$$

then

$$\sup_{t \in [0, \tau]} |X^{(N)}(t) - X(t)| \stackrel{w}{\to} 0, \ N \to \infty.$$
 (3.4)

Proof. As previously, we show that the finite dimensional distributions of $X^{(N)}(t)$ converge to those of X(t), the sequence of random variables $\{X^{(N)}(0)\}$ is tight and the sequence of processes $\{X^{(N)}(t)\}$ is tight in $C[0,\tau]$.

For any $t \in [t_{i-1}, t_i)$, $1 \le i \le N$, let $t = t_{i-1} + \xi$, where $\xi \in [0, \Delta t)$. Since r(t, s) is continuous, X is m.s. continuous so that $X^{(N)}(t) \stackrel{m.s.}{\to} X(t)$ results from

$$\begin{split} &E\Big[X^{(N)}(t)-X(t)\Big]^2\\ &=E\left[X(t_{i-1})+\frac{1}{\Delta t}\Big(X(t_i)-X(t_{i-1})\Big)(t-t_{i-1})-X(t)\Big]^2\\ &=E\left[\Big(1-\frac{\xi}{\Delta t}\Big)\Big(X(t_{i-1})-X(t_{i-1}+\xi)\Big)+\frac{\xi}{\Delta t}\Big(X(t_i)-X(t_{i-1}+\xi)\Big)\Big]^2\\ &\leq 2\Big(1-\frac{\xi}{\Delta t}\Big)^2E\Big[X(t_{i-1})-X(t_{i-1}+\xi)\Big]^2+\frac{2\xi^2}{\Delta t^2}E\Big[X(t_i)-X(t_{i-1}+\xi)\Big]^2\\ &\leq 2r(t_{i-1},t_{i-1})-4r(t_{i-1},t_{i-1}+\xi)+2r(t_{i-1}+\xi,t_{i-1}+\xi)\\ &+2r(t_i,t_i)-4r(t_i,t_{i-1}+\xi)+2r(t_{i-1}+\xi,t_{i-1}+\xi)\to 0,\ N\to\infty. \end{split}$$

This implies $(X^{(N)}(t_1),\ldots,X^{(N)}(t_n))\stackrel{m.s.}{\to} (X(t_1),\ldots,X(t_n))$ for any $n\geq 1$ and $t_1,\ldots,t_n\in[0,\tau]$ which extends to convergence in probability by Chebyshev's inequality. The latter yields the convergence of the finite dimensional distributions of $X^{(N)}(t)$ to those of X(t) as $N\to\infty$ by Theorem 18.10 in [16].

Note that the sequence $\{X^{(N)}(0)\}$ of random variables is tight, since for any $\varepsilon > 0$, there exists L such that

$$P(|X^{(N)}(0)| > L) = P(|X(0)| > L) \leq \frac{1}{L} E|X(0)| \leq \varepsilon, \ \forall N \geq 1.$$

We now show the tightness of $X^{(N)}(t)$ in $C[0, \tau]$ which, according to the second condition of Theorem 8.2, requires to show that, for any $\varepsilon, \eta > 0$,

there exists $\delta>0$ such that $P(W^{(N)}(\delta)>\epsilon)<\eta$ for all N starting from a finite value, where $W^{(N)}(\delta)=\sup_{|s-t|\leq \delta}|X^{(N)}(t)-X^{(N)}(s)|$. Given $\epsilon>0$, we have

$$\begin{split} &P\bigg(\max_{1\leq i\leq N}\sup_{t\in[t_{i-1},t_i)}|X^{(N)}(t)-X(t)|\geq\frac{\varepsilon}{3}\bigg)\\ &=P\bigg(\max_{1\leq i\leq N}\sup_{\xi\in[0,\Delta t)}\bigg|\bigg(1-\frac{\xi}{\Delta t}\bigg)\bigg(X(t_{i-1})-X(t_{i-1}+\xi)\bigg)\\ &+\frac{\xi}{\Delta t}\bigg(X(t_i)-X(t_{i-1}+\xi)\bigg)\bigg|\geq\frac{\varepsilon}{3}\bigg)\\ &\leq P\bigg(\max_{1\leq i\leq N}\sup_{\xi\in[0,\Delta t)}\bigg(1-\frac{\xi}{\Delta t}\bigg)|X(t_{i-1})-X(t_{i-1}+\xi)|\geq\frac{\varepsilon}{6}\bigg)\\ &+P\bigg(\max_{1\leq i\leq N}\sup_{\xi\in[0,\Delta t)}\frac{\xi}{\Delta t}|X(t_i)-X(t_{i-1}+\xi)|\geq\frac{\varepsilon}{6}\bigg)\\ &\leq 2P\bigg(\sup_{|s-t|<\Delta t}|X(t)-X(s)|\geq\frac{\varepsilon}{6}\bigg). \end{split}$$

This inequality implies

$$\begin{split} &P\bigg(\sup_{|s-t|\leq\delta}|X^{(N)}(t)-X^{(N)}(s)|\geq\varepsilon\bigg)\\ &=P\bigg(\sup_{|s-t|\leq\delta}|X^{(N)}(t)-X(t)+X(t)-X(s)+X(s)-X^{(N)}(s)|\geq\varepsilon\bigg)\\ &\leq P\bigg(\sup_{|s-t|\leq\delta}|X^{(N)}(t)-X(t)|+\sup_{|s-t|\leq\delta}|X(t)-X(s)|\\ &+\sup_{|s-t|\leq\delta}|X(s)-X^{(N)}(s)|\geq\varepsilon\bigg)\\ &\leq P\bigg(\max_{1\leq i\leq N}\sup_{t\in[t_{i-1},t_i)}|X^{(N)}(t)-X(t)|\geq\frac{\varepsilon}{3}\bigg)+P\bigg(\sup_{|s-t|\leq\delta}|X(t)-X(s)|\geq\frac{\varepsilon}{3}\bigg)\\ &+P\bigg(\max_{1\leq j\leq N}\sup_{s\in[t_{j-1},t_j)}|X^{(N)}(s)-X(s)|\geq\frac{\varepsilon}{3}\bigg)\\ &\leq 4P\bigg(\sup_{|s-t|\leq\Delta t}|X(t)-X(s)|\geq\frac{\varepsilon}{6}\bigg)+P\bigg(\sup_{|s-t|\leq\delta}|X(t)-X(s)|\geq\frac{\varepsilon}{3}\bigg), \end{split}$$

then if $\sup_{|s-t| \leq \delta} |X(t) - X(s)| \stackrel{w}{\to} 0$, $\delta \to 0$, we have $P(\sup_{|s-t| \leq \delta} |X^{(N)}(t) - X^{(N)}(s)| \geq \varepsilon) \to 0$, $N \to \infty$, $\delta \to 0$. Therefore $X^{(N)}(t)$ is tight on $C[0,\tau]$ by Theorem 8.2 in [17]. Further, combining with $(X^{(N)}(t_1),\dots,X^{(N)}(t_n)) \stackrel{w}{\to} (X(t_1),\dots,X(t_n))$, from Theorem 8.1 in [17], we get $\sup_{t \in [0,\tau]} |X^{(N)}(t) - X(t)| \stackrel{w}{\to} 0$, $N \to \infty$. \square

The following corollaries describe several special models that converge weakly in the continuous space $C[0,\tau]$ under some conditions. We define the finite dimensional models $X_d(t)$ and apply Theorem 3.1 to determine whether $\sup_{t\in[0,\tau]}|X_d(t)-X(t)|\stackrel{w}{\to}0$ or not.

Corollary 3.1. Let g(v), $v \ge 0$, denote the one-sided spectral density of a zero-mean weakly stationary process X(t), $0 \le t \le \tau$. Consider the sequence of processes $\{X_d(t)\}$, $0 \le t \le \tau$, which are obtained from X(t) by truncating its spectral density to $g_d(v) = g(v) \ 1(v \le v_d)$, where $v_d \ge 0$, d = 1, 2, ..., is increasing with d such that $v_d \to \bar{v}$ as $d \to \infty$. If $\bar{v} < \infty$, then

$$\sup_{t \in [0,\tau]} |X_d(t) - X(t)| \stackrel{w}{\to} 0, \ d \to \infty.$$

Proof. The FD processes $\{X_d(t)\}$ admit the spectral representations

$$X_d(t) = \int_0^{\nu_d} \left[\cos(\nu t) \, dU(\nu) + \sin(\nu t) \, dV(\nu) \right], \quad 0 \le t \le \tau, \quad d = 1, 2, \dots,$$
(3.5)

where E[dU(v)] = E[dV(v)] = 0, $E[dU(v)\,dU(v')] = E[dV(v)\,dV(v')] = g(v)\,\delta(v-v')\,dv$ and $E[dU(v)\,dV(v')] = 0$ for all $v,v'\geq 0$. The mean and variance of the uncorrelated random variables U(v) and V(v) are zero and $G(v) = \int_0^v g(\alpha)\,\alpha$, $v\geq 0$. Since $X_d(t)$ is m.s differentiable and for all $d\geq 1$,

$$E\bigg[\sup_{t\in[0,\tau]}|\dot{X}_d(t)|\bigg] = E\bigg[\sup_{t\in[0,\tau]}\bigg|\int_0^{\nu_d} -\nu\sin(\nu\,t)dU(\nu) + \nu\cos(\nu\,t)dV(\nu)\bigg|\bigg],$$

which takes the form

$$\begin{split} E \bigg[\sup_{t \in [0,\tau]} |\dot{X}_d(t)| \bigg] \\ &= E \bigg[\sup_{t \in [0,\tau]} \bigg| - v_d \sin(v_d t) U(v_d) + \int_0^{v_d} \Big(\sin(v \, t) + v t \cos(v \, t) \Big) U(v) dv \\ &+ v_d \cos(v_d \, t) V(v_d) - \int_0^{v_d} \Big(\cos(v \, t) - v t \sin(v \, t) \Big) V(v) dv \bigg| \ \bigg] \\ &\leq E \bigg[\sup_{t \in [0,\tau]} \bigg(v_d |U(v_d)| + \int_0^{v_d} (1 + v t) |U(v)| dv + v_d |V(v_d)| \\ &+ \int_0^{v_d} (1 + v t) |V(v)| dv \bigg) \bigg] \\ &\leq v_d E |U(v_d)| + \int_0^{v_d} (1 + \tau v) E |U(v)| dv + v_d E |V(v_d)| \\ &+ \int_0^{v_d} (1 + \tau v) E |V(v)| dv < \infty, \end{split}$$

by integration by parts. Then, we conclude by Theorem 3.1 that $\sup_{t\in[0,T]}|X_d(t)-X(t)|\overset{w}{\to}0$ holds. \square

Suppose that the correlation function c(u) = E[X(t+u) X(t)] of X(t) is periodic with period T > 0. Then the correlation and two-/one-sided spectral density functions of X(t) have the expressions

$$c(u) = \sum_{k = -\infty, k \neq 0}^{\infty} \frac{c_k}{2} e^{i v_k u} = \sum_{k = 1}^{\infty} c_k \cos(v_k u) \text{ and}$$

$$s(v) = \sum_{k = -\infty}^{\infty} \frac{c_k}{2} \delta(v - v_k), \quad g(v) = \sum_{k = 1}^{\infty} c_k \delta(v - v_k)$$
(3.6)

where $c_k \ge 0$, $c_k = c_{-k}$, $v_1 = 2\pi/T$ and $v_k = k v_1$, $v_k = -v_{-k}$. The series $\sum_{k=1}^{\infty} c_k$ is convergent since X(t) has finite variance by assumption. Processes with the second moment properties in (3.6) are referred to as mean square periodic. The spectral representation of X(t) has the form [24] (Section 3.9.4)

$$X(t) = \sum_{k = -\infty}^{\infty} \mathcal{V}_k e^{i v_k t} = \sum_{k = 1}^{\infty} \left[A_k \cos(v_k t) + B_k \sin(v_k t) \right], \tag{3.7}$$

where

$$\mathcal{V}_{k} = \frac{1}{T} \int_{0}^{T} X(t) e^{-iv_{k}t} dt,
A_{k} = \frac{2}{T} \int_{0}^{T} X(t) \cos(v_{k}t) dt,
B_{k} = \frac{2}{T} \int_{0}^{T} X(t) \sin(v_{k}t) dt,$$
(3.8)

and the equality in (3.7) is in the m.s. sense. The random variables in (3.8) are zero-mean, e.g.,

$$\begin{split} E[A_k] &= E \big[(2/T) \, \int_0^T X(t) \, \cos(\nu_k \, t) \, dt \big] \\ &= (2/T) \, \int_0^T E[X(t)] \, \cos(\nu_k \, t) \, dt = 0, \end{split}$$

and are uncorrelated, i.e., $E[A_k A_l] = c_k \delta_{kl}$, $E[B_k B_l] = c_k \delta_{kl}$ and $E[A_k B_l] = 0$.

The equality $\int_0^T c(s-t) \cos(v_l t) dt = (T/2) c_l \cos(v_l s), s \in [0,T]$, which results by calculations as those above, shows that $\cos(v_l t)$ is an eigenfunction of the correlation function c(u). Similar considerations show that $\sin(v_l t)$ is also an eigenfunction of c(u). The uncorrelated coefficients $\{A_k\}$ and $\{B_k\}$ are independent Gaussian variables for Gaussian processes but dependent for non-Gaussian processes. We define $X_d(t)$ by truncating the spectral representation of X(t),

$$X_d(t) = \sum_{k=1}^{d} \left[A_k \cos(v_k t) + B_k \sin(v_k t) \right], \quad d = 1, 2 \dots$$
 (3.9)

Corollary 3.2. If $\sum_{k=1}^{\infty} c_k^{1/2} < \infty$, then

$$\sup_{t \in [0,\tau]} |X_d(t) - X(t)| \stackrel{w}{\to} 0, \ d \to \infty.$$

Proof. Note that the condition $\sum_{k=1}^{\infty} c_k^{1/2} < \infty$ is not related to the frequency v_k . The eigenfunctions $\cos(v_k t)$ and $\sin(v_k t)$ lead to $L_k(\delta) = \sup_{|s-t| \le \delta} |\varphi_k(t) - \varphi_k(s)| \le 2$ for all $\delta > 0$. Since $E[A_k^2] = E[B_k^2] = c_k$ and $\sum_{k=1}^{\infty} c_k^{1/2} < \infty$ by assumption, the conditions (i) of Theorem 3.1 is satisfied so that $\sup_{t \in [0,\tau]} |X_d(t) - X(t)| \stackrel{w}{\to} 0$. \square

We now consider an extension of the previous corollary to a real-valued process $X(t),\ 0\le t\le T,$ whose correlation function is not periodic. Let

$$X^{*}(t) = X(t) 1(0 \le t \le T) + \left[X(0) \alpha(t) + X(T) \beta(t) \right] 1(T < t \le T^{*}),$$

$$0 \le t \le T^{*},$$
(3.10)

be a extension of X(t) to the time interval $[0,T^*]$, where $T^*=T+\Delta$, $\Delta>0$ is arbitrary, $\alpha(t)=(t-T)/\Delta$ and $\beta(t)=1-\alpha(t)$. The periodic extension of $X^*(t)$ to the real line is also denoted by $X^*(t)$ for simplicity. This extension has periodic samples with period $T^*=T+\Delta$ and $X^*(0)=X^*(T^*)$ a.s. It is not weakly stationary even if X(t) is weakly stationary since its correlation function $c^*(s,t)=E\left[X^*(s)X^*(t)\right]$ depends on the times s and t, e.g., $c^*(s,t)=E\left[\left(X(0)\alpha(s)+X(T)\beta(s)\right)X(t)\right]=\alpha(s)\,c(t)+\beta(s)\,c(t-T)$ for $s\in[T,T^*]$ and $t\in[0,T]$. We note that any other continuous extension of the samples of X(t) on [0,T] to samples of $X^*(t)$ on $[0,T^*]$ can be used provided it is periodic with period T^* . Since almost all samples of X(t) are continuous on [0,T] by assumption and the samples of $X^*(t)$ are continuous and periodic with period T^* by construction, the Fourier series representations of the samples of $X^*(t)$ converge absolutely and uniformly [25] (Section 1.10). These series have the form

$$X^*(t) = A_0^*/2 + \sum_{k=1}^{\infty} \left[A_k^* \cos(\nu_k t) + B_k^* \sin(\nu_k t) \right], \quad t \in [0, T^*],$$
 (3.11)

where $v_1 = 2 \pi / T^*$, $v_k = k v_1$ and

$$A_k^* = \frac{2}{T^*} \int_0^{T^*} X^*(t) \cos(\nu_k t) dt, \quad k = 0, 1, 2, ...,$$

$$B_k^* = \frac{2}{T^*} \int_0^{T^*} X^*(t) \sin(\nu_k t) dt, \quad k = 1, 2,$$
(3.12)

We define $X_d^*(t)$ by truncating the spectral representation of $X^*(t)$,

$$X_d^*(t) = A_0^*/2 + \sum_{k=1}^d \left[A_k^* \cos(\nu_k t) + B_k^* \sin(\nu_k t) \right], \quad d = 1, 2, \dots$$
 (3.13)

Corollary 3.3. If
$$\sum_{k=1}^{\infty} \left(E\left[(A_k^*)^2 \right]^{1/2} + E\left[(B_k^*)^2 \right]^{1/2} \right) < \infty$$
, then
$$\sup_{t \in [0,\tau]} |X_d^*(t) - X^*(t)| \stackrel{w}{\to} 0, \ d \to \infty.$$

Proof. We cannot apply Corollary 3.2, because the models in (3.7) and (3.10) differ, e.g., $X^*(t)$ is not stationary. We first show that $X_d^*(t)$ converges to $X^*(t)$ in mean square sense. For any m > n, we have

$$\begin{split} &E\left[X_{n}^{*}(t)-X_{m}^{*}(t)\right]^{2}=E\left[\sum_{k=n+1}^{m}\left[A_{k}^{*}\cos(v_{k}t)+B_{k}^{*}\sin(v_{k}t)\right]^{2}\right]\\ &\leq2E\left[\sum_{k=n+1}^{m}A_{k}^{*}\cos(v_{k}t)\right]^{2}+2E\left[\sum_{k=n+1}^{m}B_{k}^{*}\sin(v_{k}t)\right]^{2}\\ &\leq2\sum_{k=n+1}^{m}\left(E\left[(A_{k}^{*})^{2}\right]+E\left[(B_{k}^{*})^{2}\right]\right)\\ &+4\sum_{n+1\leq i< j\leq m}\left(E\left[A_{k}^{*}A_{j}^{*}\right]\cos(v_{i}t)\cos(v_{j}t)+E\left[B_{i}^{*}B_{j}^{*}\right]\sin(v_{i}t)\sin(v_{j}t)\right)\\ &\leq2\sum_{k=n+1}^{m}\left(E\left[(A_{k}^{*})^{2}\right]+E\left[(B_{k}^{*})^{2}\right]\right)\\ &+4\sum_{n+1\leq i< j\leq m}\left(E\left[(A_{i}^{*})^{2}\right]^{1/2}E\left[(A_{j}^{*})^{2}\right]^{1/2}+E\left[(B_{i}^{*})^{2}\right]^{1/2}E\left[(B_{j}^{*})^{2}\right]^{1/2}\right)\\ &=2\left(\sum_{k=n+1}^{m}E\left[(B_{k}^{*})^{2}\right]^{1/2}\right)^{2}+2\left(\sum_{k=n+1}^{m}E\left[(B_{k}^{*})^{2}\right]^{1/2}\right)^{2}. \end{split}$$

This shows that $\{X_d^*(t)\}$ is Cauchy, since $\sum_{k=1}^\infty E\left[(A_k^*)^2\right]^{1/2} < \infty$ and $\sum_{k=1}^\infty E\left[(B_k^*)^2\right]^{1/2} < \infty$ so that $X_d^*(t) \xrightarrow{m.s.} X^*(t)$, which implies the convergence of the finite dimensional distributions of $X_d^*(t)$ to those of $X^*(t)$. Further, by Theorem 3.1 the sequence of processes $\{X_d^*(t)\}$ has the property $\sup_{t \in [0,\tau]} |X_d^*(t) - X^*(t)| \xrightarrow{\omega} 0$, since $\sum_{k=1}^\infty \left(E\left[(A_k^*)^2\right]^{1/2} + E\left[(B_k^*)^2\right]^{1/2}\right) < \infty$. \square

4. Examples

We illustrate numerically that samples and extremes of real-valued continuous processes X(t) can be approximated by samples of FD models $\{X_d(t)\}$, d=1,2,..., of these processes for sufficiently large d provided that they satisfy the conditions of Theorem 3.1 and related results. The discrepancy between samples of X(t) and $X_d(t)$ is measured by the metric $\sup_{0 \le t \le \tau} |X(t,\omega) - X_d(t,\omega)|$ of the space $C[0,\tau]$ of continuous samples. This discrepancy cannot be obtained exactly since the samples of these processes can only be recorded at finite numbers of times, e.g., the times $\{t_k\}$, k=0,1,...,N, where $t_k=t_{k-1}+\Delta t$ and $\Delta t=\tau/N$. The numerical value, $\max_{k=0,1,...,N}|X(t_k,\omega) - X_d(t_k,\omega)|$, of the discrepancy between X(t) and $X_d(t)$ provides a lower bound on $\sup_{0 \le t \le \tau}|X(t,\omega) - X_d(t,\omega)|$. Since X(t) and $X_d(t)$ have continuous samples, it is expected that the lower bound is tight for sufficiently large

Accordingly, we approximate the samples of X(t) by those of random vectors $\left(X(t_0),X(t_1)\dots,X(t_N)\right)$, and the actual discrepancy $\sup_{0\leq t\leq \tau}|X(t,\omega)-X_d(t,\omega)|$ between samples of X(t) and $X_d(t)$ by its numerical values $\max_{k=0,1,\dots,N}|X(t_k,\omega)-X_d(t_k,\omega)|$ for large N. In some of examples, we only prove the weak convergence of X_d to X in $C[0,\tau]$. Under this convergence, the measure of the set

$$\varOmega_d(\varepsilon) = \{\omega : \sup_{0 \le t \le \tau} |X(t,\omega) - X_d(t,\omega)| > \varepsilon\}$$

can be made as small as desired for any $\varepsilon > 0$ by increasing d. Generally, the sets $\Omega_d(\varepsilon)$ differ for $d \neq d'$ but have small measures for sufficiently large d and d'. Therefore, although we may not have almost sure convergence, we can still use the samples of $X_d(t)$ as substitutes for samples of X(t) for sufficiently large d, since the probability that samples of $X_d(t)$ may misrepresent samples of X(t) is $P(\Omega_d(\varepsilon))$.

This section illustrates the construction of FD models $X_d(t)$ for three real-valued processes X(t), a stationary Gaussian process, a non-stationary Gaussian process and a non-Gaussian translation process, and (2) quantifies the performance of the resulting FD models $X_d(t)$ by two metrics, the norm $\sup_{0 \le t \le \tau} |X(t) - X_d(t)|$ and the discrepancy between extremes $\sup_{0 \le t \le \tau} |X(t)|$ and $\sup_{0 \le t \le \tau} |X_d(t)|$ of X(t) and $X_d(t)$. The examples show that under the conditions of our theoretical results, samples and extremes of $X_d(t)$ can be used as substitutes for samples and extremes of X(t) provided that the stochastic dimension d is sufficiently large.

Example 4.1. Let X(t), $0 \le t \le \tau$, be a real-valued process defined by the differential equation

$$\ddot{X}(t) + \alpha \dot{X}(t) + \beta X(t) = Y(t), \quad 0 \le t \le \tau, \tag{4.1}$$

with the initial conditions X(0)=0 and $\dot{X}(0)=0$, where $\alpha, \beta>0$ are constants, Y is the stationary solution of $dY(t)=-\rho\,Y(t)\,dt+\sqrt{2\,\rho}\,d\,B(t)$, $\rho>0$, and B denotes the standard Brownian motion.

The mean and correlation functions of Y(t) are E[Y(t)] = 0 and $E[Y(s)Y(t)] = \exp(-\rho |s-t|)$ for any $\rho > 0$. Since the Brownian motion has continuous samples, the processes X(t), $\dot{X}(t)$ and Y(t) also have continuous samples as they are obtained from samples of B(t) by integration. These processes are Gaussian as linear transformations of B(t). The target process is the solution X(t) of (4.1) which is a non-stationary Gaussian process with continuous samples.

The basis functions $\{\varphi_k(t)\}\$ for the FD models $X_d(t)$ of X(t) in (4.1) are the top eigenfunctions of the correlation function c(s,t)=

 $E[X(s)\,X(t)]$ of X(t), i.e., the eigenfunctions corresponding to the largest d eigenvalues of c(s,t), $0\leq s,t\leq \tau$. The correlation function of X(t) can be obtained by solving the differential equations for the correlation function of the vector-valued process $\left(X(t),\dot{X}(t),Y(t)\right)$, see [24], Section 7.2.1.1, or by estimation from samples of X(t). The basis functions $\{\varphi_k(t)\}$ were obtained by (A.1) in Appendix. FD models of X(t) can also be obtained from FD models $B_d(t)$ of the Brownian motion B(t) and the defining equation of X(t) but this approach was not followed.

We first show that samples of X(t) can be approximated by samples of $X_d(t)$ for sufficiently large d, then present numerical estimates for the discrepancy between samples of X(t) and $X_d(t)$. The mean square (m.s.) convergence $X_d(t) \stackrel{\text{m.s.}}{\to} X(t)$ for a fixed time t follows from Mercer's theorem. This also implies the m.s. convergence of $\left(X_d(s_1), \ldots, X_d(s_m)\right)$ to $\left(X(s_1), \ldots, X(s_m)\right)$ as $d \to \infty$ for arbitrary $0 \le s_1 < \cdots < s_m \le \tau$ and $m \ge 1$, then their convergence also hold in probability by Chebyshev's inequality, which leads to the convergence of the finite dimensional distributions of $X_d(t)$ to those of X(t), see [16], Theorem 18.10. Since the process X(t) is Gaussian with zero mean and finite variance, we also have the a.s. convergence of X_d to X in $C[0,\tau]$, see Theorem 3.2. Accordingly, we can substitute samples of X(t) with samples of $X_d(t)$ for sufficiently large d.

The following numerical results are for $\alpha=0.1$, $\beta=25$, $\rho=5$, $\tau=10$ and the time step $\Delta t=\tau/N=0.01$ with N=1000. The solid and dotted lines of Fig. 3 show five samples of X(t) and the corresponding samples of $X_d(t)$ for d=5, 15 and 25 (left, middle and right panels). Histograms of the first metric $\sup_{0 \le t \le \tau} |X(t) - X_d(t)|$ are in Fig. 4 for the same values of d. Figs. 5 and 6 focus on the second metric. They show scatter plots of $\sup_{0 \le t \le \tau} |X(t)|$, $\sup_{0 \le t \le \tau} |X_d(t)|$ and histograms of $\sup_{0 \le t \le \tau} |X(t)| - \sup_{0 \le t \le \tau} |X_d(t)|$ for t=0, 15 and 25 (left, middle and right panels). The plots in Figs. 4–6 show, in agreement with our theoretical results, that the discrepancy between samples and extremes of t=0 and t=0 and t=0 are the stochastic dimension t=0. The plots in these figures are based on 1000 samples of t=0 and t=0.

Example 4.2. Let X(t) be a zero-mean stationary Gaussian process with spectral density $g(v) = \sum_{k=1}^{\infty} c_k \, \delta(v - v_k)$, where $c_k = \alpha \, \int_{I_k} (v^2 + \rho^2)^{-1-\kappa} \, dv$, $I_k = [v_k - \Delta v/2, v_k + \Delta v/2]$, $v_k = (k-1/2) \, \Delta v$, k = 1, 2, ..., $\Delta v > 0$ denotes the frequency increment, $\kappa > 0$, $\rho \ge 0$ and $\alpha = \frac{2(2\kappa)!!\rho^{1+2\kappa}}{(2\kappa-1)!!\pi}$ such that $\sum_{k=1}^{\infty} c_k = 1$.

The sequence of processes $X_d(t)$ has the form in (3.9) so that $\sup_{t\in[0,\tau]}|X_d(t)-X(t)|\overset{w}{\to}0$, since

$$\begin{split} \sum_{k=2}^{\infty} c_k^{1/2} &= \sum_{k=2}^{\infty} \left(\int_{\nu_k - \Delta \nu/2}^{\nu_k + \Delta \nu/2} \frac{\alpha}{(\nu^2 + \rho^2)^{1 + \kappa}} d\nu \right)^{1/2} \leq \sum_{k=2}^{\infty} \frac{\alpha^{1/2} \Delta \nu^{1/2}}{(\nu_k - \Delta \nu/2)^{1 + \kappa}} \\ &\leq \sum_{k=2}^{\infty} \frac{\Delta \nu^{-1/2 - \kappa} \alpha^{1/2}}{(k-1)^{1 + \kappa}} < \infty. \end{split}$$

This implies $\sup_{t \in [0,\tau]} |X_d(t) - X(t)| \stackrel{a.s.}{\to} 0$ by Theorem 3.2 since $X_d(t)$ and X(t) are Gaussian processes. Hence, samples of X(t) can be substituted with samples of $X_d(t)$ for sufficiently large d.

As previously stated, since it is not possible to generate the samples of target process X(t), we approximate this process by $X_{\vec{n}}(t)$, which is set equal to $X_d(t)$ in (3.9) with d replaced by $\bar{n}\gg d$. The following numerical results are for $\rho=5$, $\tau=10$, $\kappa=2$, $\bar{n}=1000$, the frequency increments $\Delta v=0.1$ and the time step $\Delta t=\tau/N=0.01$ with N=1000. The plots in Figs. 7, 8, 9 and 10 are similar to those in Figs. 3, 4, 5 and 6 of the previous example. The solid and dotted lines of Fig. 7 show five samples of X(t) and the corresponding samples of $X_d(t)$ for d=50, 100 and 150 (left, middle and right panels). Histograms of the first metric $\sup_{0 \le t \le \tau} |X(t) - X_d(t)|$ are in Fig. 8 for the same values of d. Figs. 9 and 10 focus on the second metric. They show scatter plots of $\sup_{0 \le t \le \tau} |X(t)|$, $\sup_{0 \le t \le \tau} |X_d(t)|$ and histograms of $\sup_{0 \le t \le \tau} |X_d(t)| - \sup_{0 \le t \le \tau} |X_d(t)|$ for d=50, 100 and 150 (left, middle

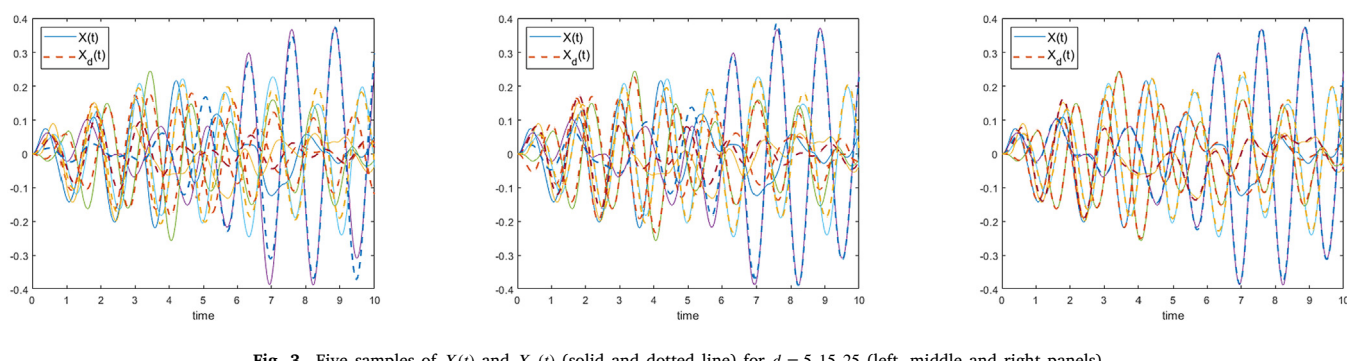


Fig. 3. Five samples of X(t) and $X_d(t)$ (solid and dotted line) for d = 5, 15, 25 (left, middle and right panels).

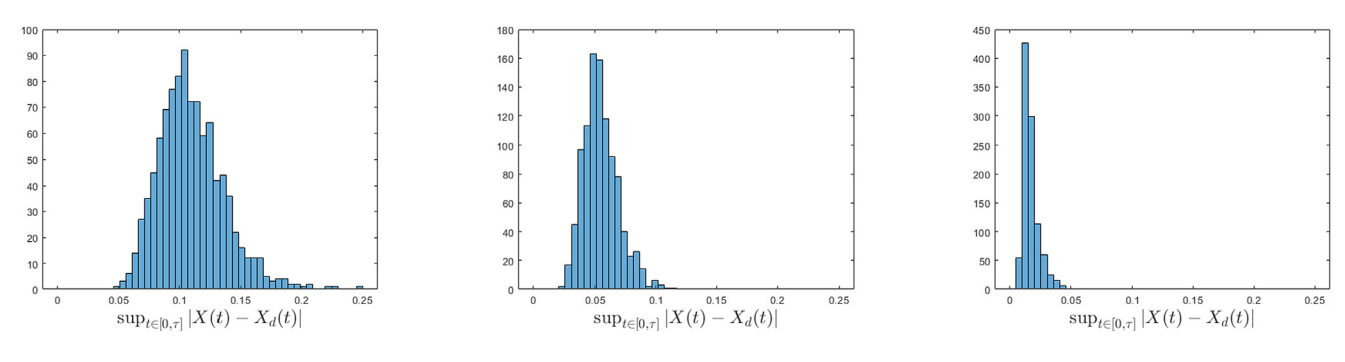


Fig. 4. Histograms of $\sup_{t \in [0,r]} |X(t) - X_d(t)|$ for d = 5, 15, 25 (left, middle and right panels) based on 1000 samples.

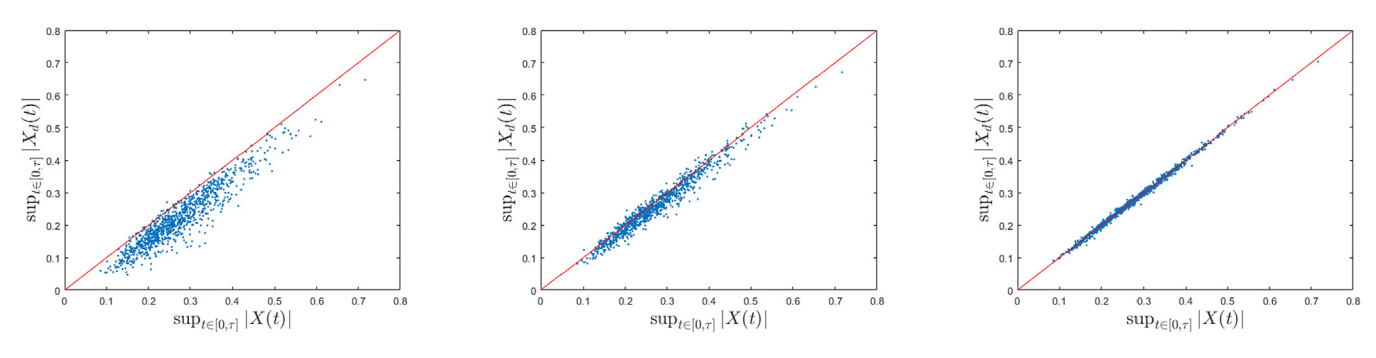


Fig. 5. Scatter plots of $\sup_{t \in [0,\tau]} |X(t)|$ and $\sup_{t \in [0,\tau]} |X_d(t)|$ for d = 5, 15, 25 (left, middle and right panels).

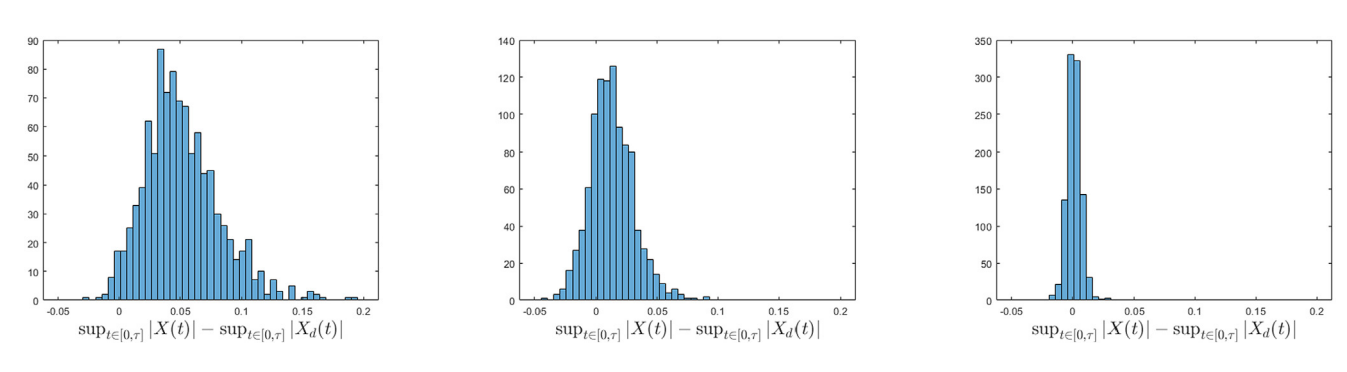


Fig. 6. Histograms of $\sup_{t \in [0,\tau]} |X(t)| - \sup_{t \in [0,\tau]} |X_d(t)|$ for d = 5, 15, 25 (left, middle and right panels) based on 1000 samples.

and right panels). The plots in Figs. 8-10 show, in agreement with our theoretical results, that the discrepancy between samples and extremes of X(t) and $X_d(t)$ can be made as small as desired by increasing the stochastic dimension d. The plots in these figures are based on 1000 samples of X(t) and $X_d(t)$.

Example 4.3. Suppose a sample $(X(t_0), X(t_1), \dots, X(t_N))$ of a realvalued process X(t), $0 \le t \le \tau$, with continuous samples is available.

Our objectives are to construct the law of X(t), develop FD models $\{X_d(t)\}$ for this process, and determine whether X_d converges weakly/a.s. to X in the space of continuous functions. These objectives can be achieved under the assumptions that (1) the target X(t) is an ergodic translation process and (2) the available sample of X(t) is sufficiently long such it is possible to construct accurate estimates \hat{F} of the marginal distribution F of X(t) and of the correlation function of the Gaussian image G(t) of X(t).

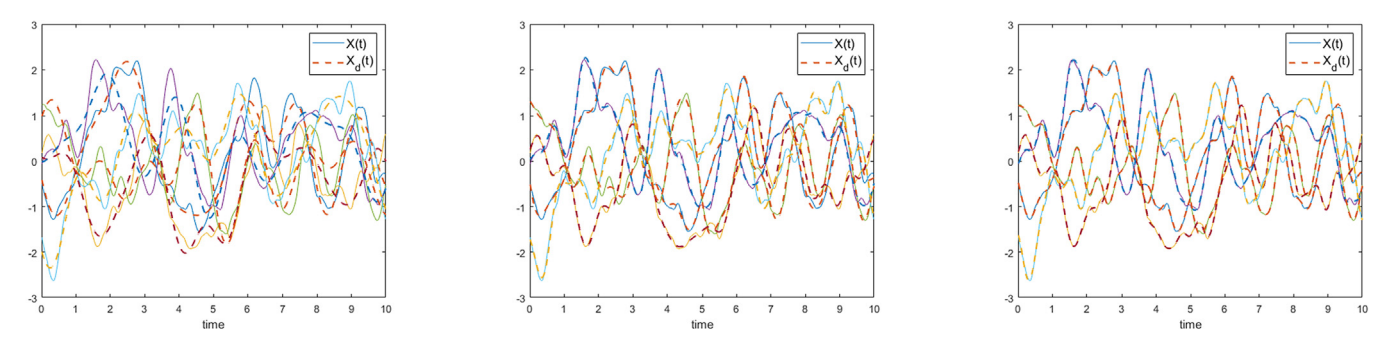


Fig. 7. Five samples of X(t) and $X_d(t)$ (solid and dotted line) for d = 50, 100, 150 (left, middle and right panels).

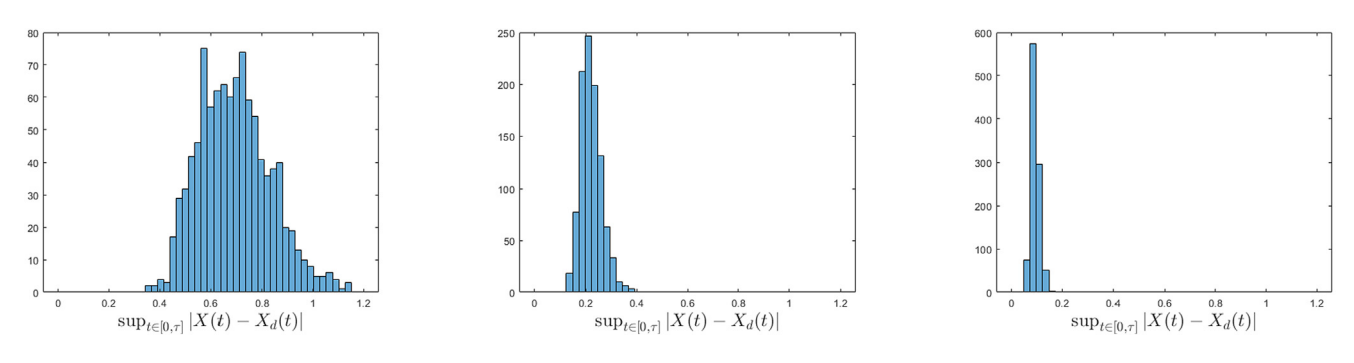


Fig. 8. Histograms of $\sup_{t \in [0, \tau]} |X(t) - X_d(t)|$ for d = 50, 100, 150 (left, middle and right panels) based on 1000 samples.

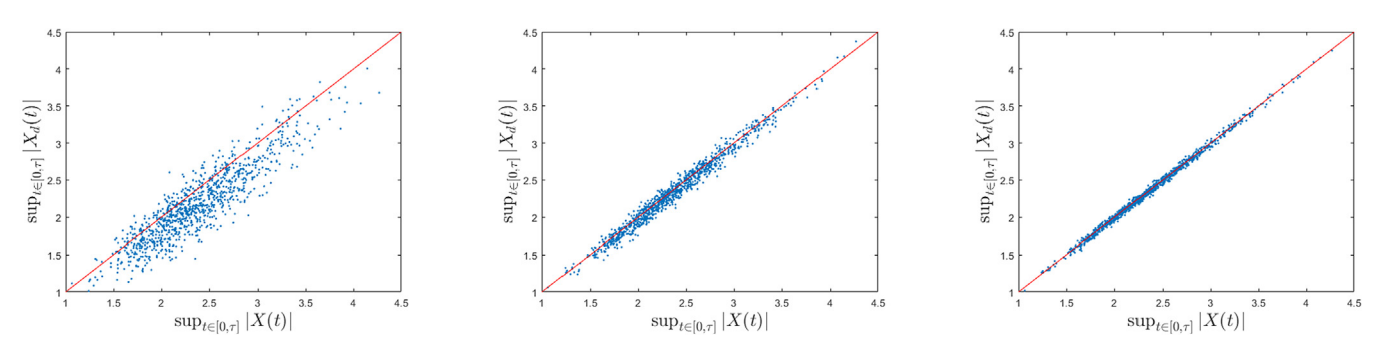


Fig. 9. Scatter plots of $\sup_{t \in [0,\tau]} |X(t)|$ and $\sup_{t \in [0,\tau]} |X_d(t)|$ for d = 50,100,150 (left, middle and right panels).

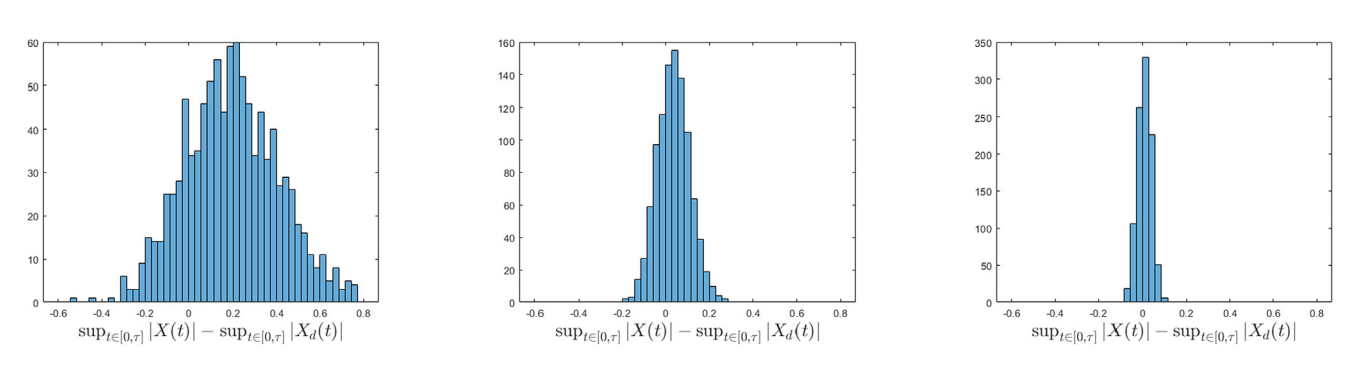


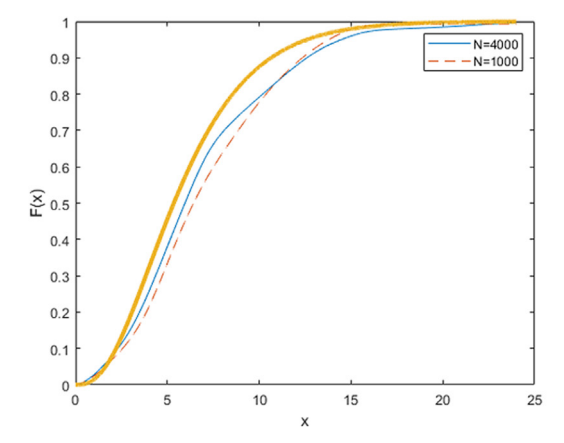
Fig. 10. Histograms of $\sup_{t \in [0,\tau]} |X(t)| - \sup_{t \in [0,\tau]} |X_d(t)|$ for d = 50,100,150 (left, middle and right panels) based on 1000 samples.

We proceed as follows. First, the sample of X(t) is used to estimate the marginal distribution F of X(t) and, then, construct the corresponding samples of its Gaussian image by $\hat{G}(t) = \Phi^{-1} \circ \hat{F} \left(X(t) \right)$, where \hat{F} is an estimate of F delivered by the MATLAB function ksdensity. Second, the resulting sample of $\hat{G}(t)$ is used to estimate its correlation function $\hat{c}(u) = E[\hat{G}(t+u)\,\hat{G}(t)]$. This estimate and the standard Gaussian distribution Φ define completely the law of $\hat{G}(t)$. Third, the law of $\hat{G}(t)$

is used to construct FD models $\{\hat{G}_d(t)\}$ of the type in (2.3), i.e.,

$$\hat{G}_d(t,\omega) = \sum_{k=1}^d \hat{\lambda}_k^{1/2} \hat{Z}_k(\omega) \hat{\varphi}_k(t), \tag{4.2}$$

where $\{\hat{\lambda}_k, \hat{\varphi}_k\}$ denote the eigenvalues and the eigenfunctions of the correlation function of $\hat{G}(t)$ and the samples $\hat{Z}_k(\omega)$ of \hat{Z}_k are obtained by projecting the samples $\hat{G}(t, \omega)$ on the eigenfunctions $\hat{\varphi}$ in $[0, \tau]$. The



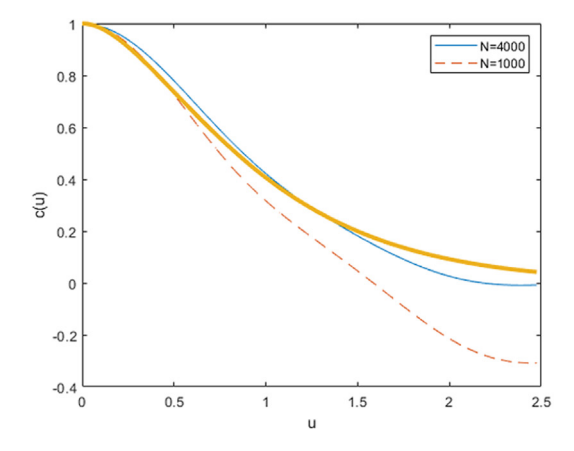
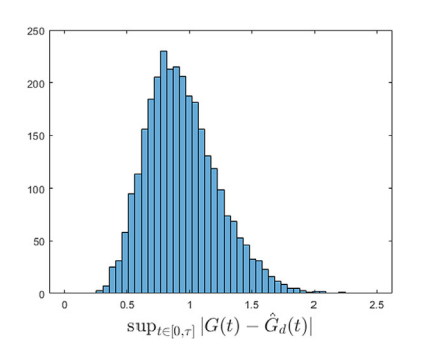
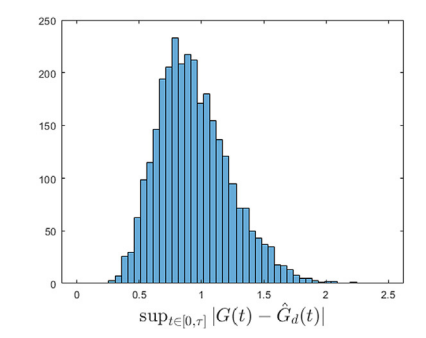


Fig. 11. Distributions F and \hat{F} of X(t) (left panel) and correlation functions c and \hat{c} of G(t) (right panel). The heavy solid lines are the target distribution and correlation function. The thin solid and heavy dotted lines are corresponding estimates based on samples of length N = 1000 and N = 4000.





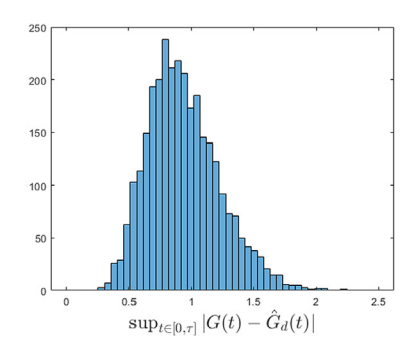
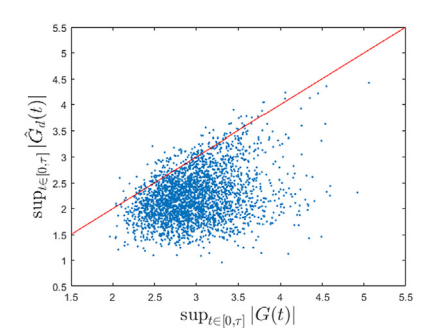
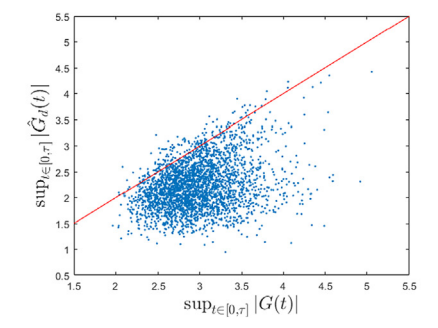


Fig. 12. Histograms of $\sup_{t \in [0,\tau]} |G(t) - \hat{G}_d(t)|$ for N = 1000 and d = 100, 150, 200 (left, middle and right panels) based on 3000 samples.





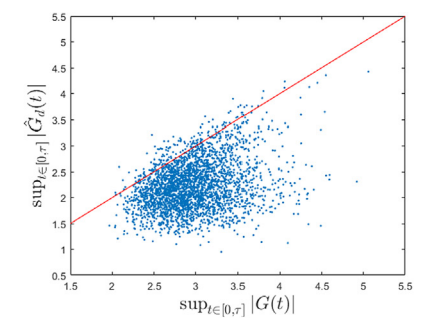


Fig. 13. Scatter plots of $\sup_{t \in [0, \tau]} |G(t)|$ and $\sup_{t \in [0, \tau]} |\hat{G}_d(t)|$ for N = 1000 and d = 100, 150, 200 (left, middle and right panels) based on 3000 samples.

corresponding FD model of $\hat{X}(t)$ is the same as in Theorem 3.3, i.e., $\hat{X}_d(t,\omega) = \hat{F}^{-1} \circ \Phi(\hat{G}_d(t,\omega))$.

Note that G(t) has zero mean. If G(t) has continuous samples and continuous correlation function, then (Theorem 3.2)

$$\sup_{t \in [0,\tau]} |\hat{G}_d(t) - \hat{G}(t)| \xrightarrow{a.s.} 0 \text{ and } \sup_{t \in [0,\tau]} |\hat{X}_d(t) - \hat{X}(t)| \xrightarrow{a.s.} 0, \quad d \to \infty,$$

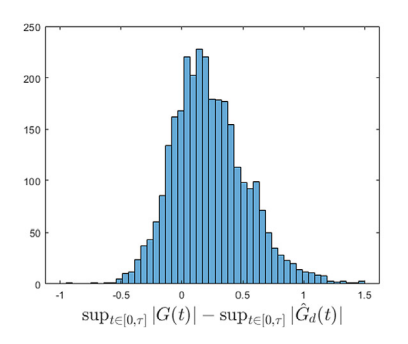
where the latter statement follows by Theorem 3.3 provided that \hat{F} is continuous and strictly monotonically increasing.

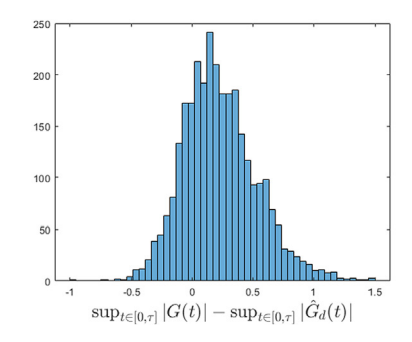
In fact, G(t) is a zero-mean, unit-variance stationary Gaussian process with one-sided spectral density $g(v) = \alpha (4\rho^3/\pi)/(v^2+\rho^2)^2$ truncated at $\bar{v}=5$, where $\alpha=1.0232$. The following numerical results are for $\tau=100$, $\Delta v=0.025$, $\Delta t=0.025$, $\rho=2$ and a Gamma distribution $F(x)=\gamma(k,x/\theta)/\Gamma(k)$ with k=3 and $\theta=2$, where $\gamma(\cdot,\cdot)$ is the lower incomplete gamma function. We consider two samples of X(t) with length N, where N=1000 and N=4000.

The heavy solid line in the left panel of Fig. 11 is the actual distribution F of X(t). The thin solid and dashed lines are the estimates

 \hat{F} of F based on the samples of this process of length N=1000 and N=4000. The right panel of the figure shows the correlation function c(u)=E[G(t+u)G(t)] (heavy solid line) and its estimates $\hat{c}(u)=E[\hat{G}(t+u)\hat{G}(t)]$ (thin solid and dashed lines). As expected, the estimates improve with the sample size.

The following figures quantify the performance of the FD models constructed from the available two samples of length N=1000 (Figs. 12–14) and N=4000 (Figs. 15–17). All plots are based on 3000 samples. Histograms of the first metric $\sup_{t\in[0,\tau]}|G(t)-\hat{G}_d(t)|$ are in the left, middle and right panels of Fig. 12 for d=100,150,200. Figs. 13 and 14 focus on the second metric. They show scatter plots of $\left(\sup_{0\leq t\leq \tau}|G(t)|,\sup_{0\leq t\leq \tau}|\hat{G}_d(t)|\right)$ and histograms of $\sup_{0\leq t\leq \tau}|G(t)|-\sup_{0\leq t\leq \tau}|\hat{G}_d(t)|$ for d=100,150 and 200 (left, middle and right panels). Fig. 15, 16 and 17 show the same statistics as in Figs. 12–14 but for N=4000. The same types of plots are in Figs. 18–20 but the FD model $G_d(t)$ is based on the actual law of G(t) rather than estimates of it. The plots show that $G_d(t)$ is superior to the FD models $\hat{G}_d(t)$ based on a single sample of the target process, an expected result





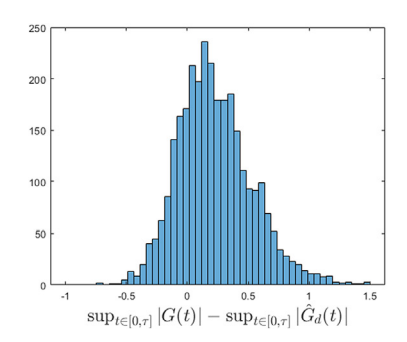
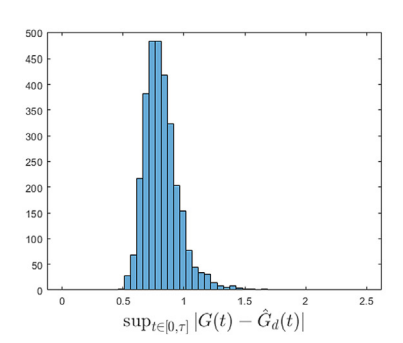
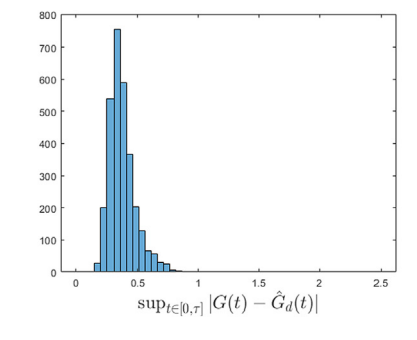


Fig. 14. Histograms of $\sup_{t\in[0,\tau]}|G(t)|$ – $\sup_{t\in[0,\tau]}|\hat{G}_d(t)|$ for N=1000 and d=100,150,200 (left, middle and right panels) based on 3000 samples.





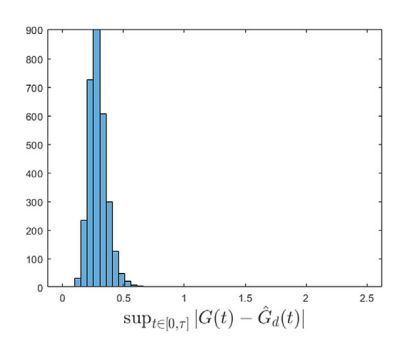
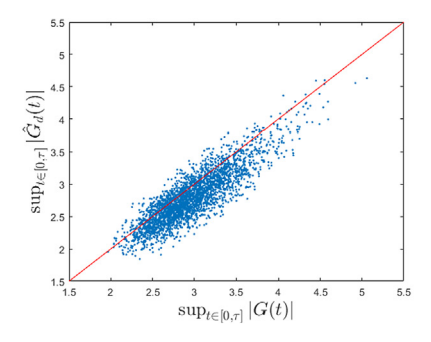
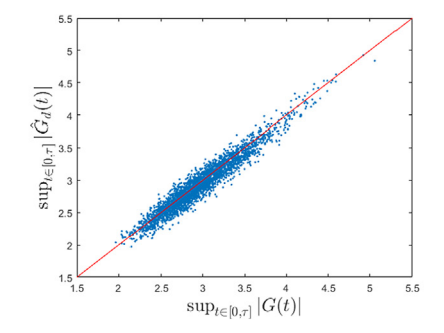


Fig. 15. Histograms of $\sup_{t \in [0, \tau]} |G(t) - \hat{G}_d(t)|$ for N = 4000 and d = 100, 150, 200 (left, middle and right panels) based on 3000 samples.





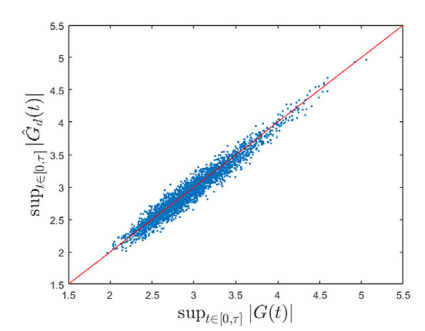
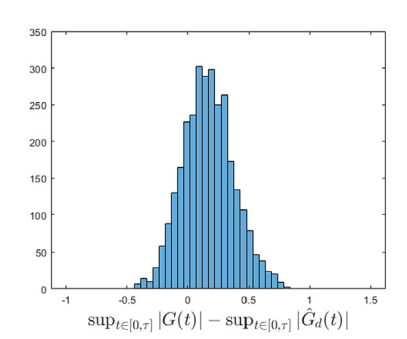
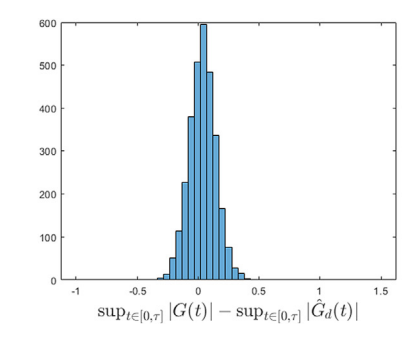


Fig. 16. Scatter plots of $\sup_{t \in [0,\tau]} |G(t)|$ and $\sup_{t \in [0,\tau]} |\hat{G}_d(t)|$ for N = 4000 and d = 100, 150, 200 (left, middle and right panels) based on 3000 samples.





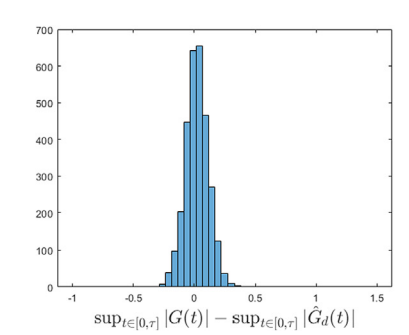
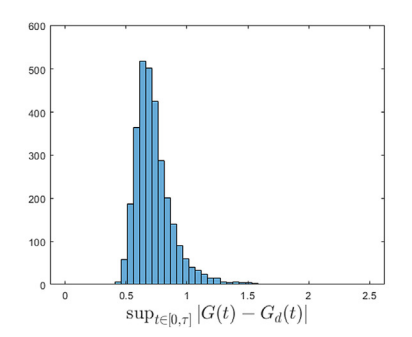


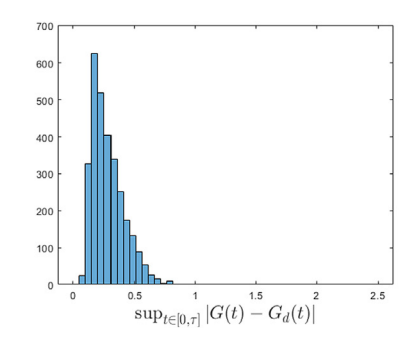
Fig. 17. Histograms of $\sup_{t \in [0,\tau]} |G(t)| - \sup_{t \in [0,\tau]} |\hat{G}_d(t)|$ for N = 4000 and d = 100, 150, 200 (left, middle and right panels) based on 3000 samples.

since $\hat{G}_d(t)$ is constructed from approximate Gaussian samples and basis functions based on estimates \hat{F} and $\hat{c}(u)$ of the actual distribution F and correlation function c(u) whose accuracy depends on the sample size. Also, as expected, the performance of the FD model $\hat{G}_d(t)$ improves with the sample size. The plots also show that under adequate statistical information on the target process and sufficiently large d, samples and extremes of X(t) can be approximated by those of $X_d(t)$.

5. Comments

Finite dimensional (FD) models $X_d(t)$, d=1,2,..., i.e., deterministic functions of time which depend on finite sets of $d<\infty$ random variables, have been developed for real-valued processes X(t) with finite variances and continuous samples defined on bounded intervals $[0,\tau]$. It was shown that under some conditions the discrepancy $\sup_{t\in[0,\tau]}|X(t)-X_d(t)|$ between samples of target processes X(t) and their FD models can be made as small as desired by increasing the





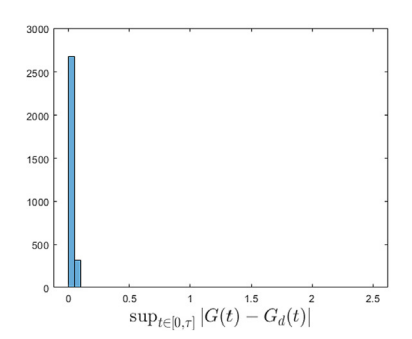
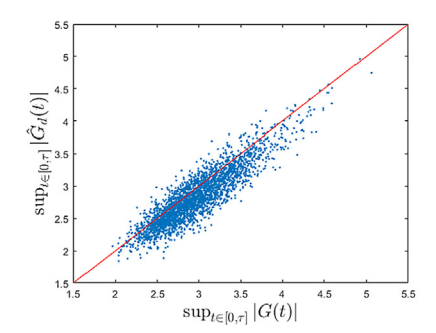
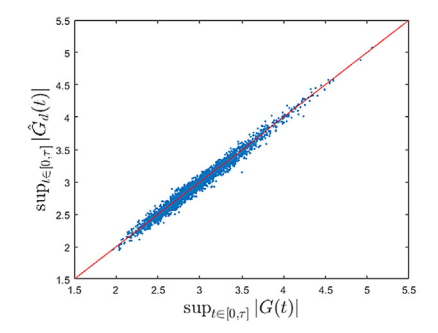
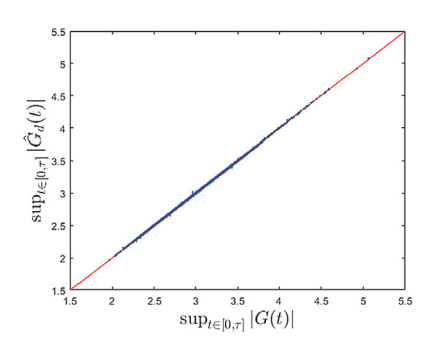


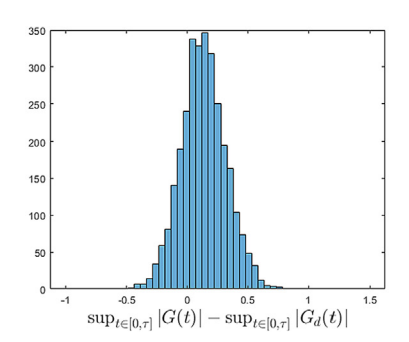
Fig. 18. Histograms of $\sup_{t \in [0,\tau]} |G(t) - G_d(t)|$ for d = 100, 150, 200 (left, middle and right panels) based on 3000 samples.

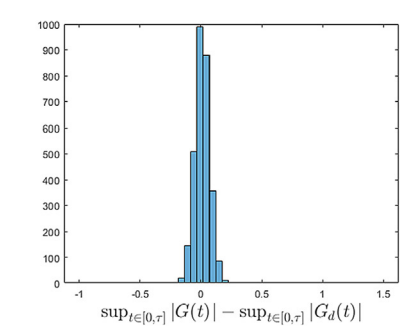


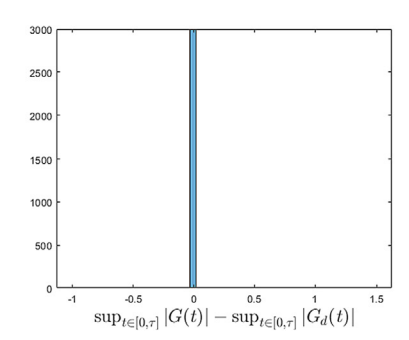




 $\textbf{Fig. 19.} \hspace{0.2cm} \textbf{Scatter plots of } \sup_{t \in [0,\tau]} |G(t)| \hspace{0.2cm} \textbf{and} \hspace{0.2cm} \sup_{t \in [0,\tau]} |G_d(t)| \hspace{0.2cm} \textbf{for} \hspace{0.2cm} d = 100, 150, 200 \hspace{0.2cm} \textbf{(left, middle and right panels)} \hspace{0.2cm} \textbf{based on 3000 samples.} \\$







 $\textbf{Fig. 20.} \ \ \text{Histograms of } \sup_{t \in [0,\tau]} |G(t)| - \sup_{t \in [0,\tau]} |G_d(t)| \ \ \text{for } d = 100, 150, 200 \ \ \text{(left, middle and right panels) based on 3000 samples.}$

stochastic dimension d. Under these conditions and sufficiently large d, samples of X(t) can be approximated by samples of $X_d(t)$ so that extremes of X(t) can be approximated by those of $X_d(t)$. The discrepancy between these samples is measured by the metric of the space $C[0,\tau]$ of real-valued continuous functions defined on $[0,\tau]$. Examples are presented to illustrate numerically and graphically the relationship between samples of X(t) and $X_d(t)$.

Declaration of competing interest

The authors declare that they have no known competing financial interests or personal relationships that could have appeared to influence the work reported in this paper.

Data availability

The datasets generated during the current study are not publicly available, since they have been generated for particular applications, but are available from the corresponding author on reasonable request.

Acknowledgment

The work reported in this paper has been partially supported by the National Science Foundation, USA under the grant CMMI-2013697. This support is gratefully acknowledged.

Appendix

Covariance function of **X**(t) in Example 4.1 Let $x(t) = (x_1(t), x_2(t), x_3(t))^T$ and $x_1(t) = X(t), x_2(t) = \dot{X}(t), x_3(t) = Y(t)$. The covariance function $r(t, s) = E[x(t)x(s)^T]$ of x(t) can be obtained in two steps. First, we calculate the covariance matrix r(t, t) of the random vector x(t), $t \ge 0$, from

$$\dot{r}(t,t) = ar(t,t) + r(t,t)a^T + bb^T,$$

where

$$r(0,0) = \mathbf{0}, \ a = \left[egin{array}{ccc} 0 & 1 & 0 \\ -eta & -lpha & 1 \\ 0 & 0 & -
ho \end{array}
ight], \ b = \left[egin{array}{c} 0 \\ 0 \\ \sqrt{2
ho} \end{array}
ight].$$

The solution of this ordinary differential equation is

$$R(t) = -A^{-1}B + e^{At}A^{-1}B,$$

where $R(t) = (r_{11}(t, t), r_{12}(t, t), r_{13}(t, t), r_{22}(t, t), r_{23}(t, t), r_{33}(t, t))^T$,

$$A = \begin{bmatrix} 0 & 2 & 0 & 0 & 0 & 0 \\ -\beta & -\alpha & 1 & 1 & 0 & 0 \\ 0 & 0 & -\rho & 0 & 1 & 0 \\ 0 & -2\beta & 0 & -2\alpha & 2 & 0 \\ 0 & 0 & -\beta & 0 & -\rho -\alpha & 1 \\ 0 & 0 & 0 & 0 & 0 & -2\alpha \end{bmatrix}$$

and $B = (0, 0, 0, 0, 0, 2\rho)^T$.

Then, we calculate the correlation function r(t, s) of the vectorvalued process x(t) from

$$\frac{\partial r(t,s)}{\partial t} = ar(t,s), \quad t > s > 0,$$

for t > s > 0 and the initial condition r(s, s), which is available from the previous step. The solution of this equation has the form

$$r(t,s) = e^{Dt}g(s), \ t > s \ge 0,$$

where g(s) is any deterministic function so that

$$r(t,s) = e^{D(t-s)}(-TA^{-1}B + Te^{As}A^{-1}B), \ t > s \ge 0,$$
(A.1)

where

$$D = \begin{bmatrix} 0 & 0 & 0 & 1 & 0 & 0 & 0 & 0 & 0 \\ 0 & 0 & 0 & 0 & 1 & 0 & 0 & 0 & 0 \\ 0 & 0 & 0 & 0 & 0 & 1 & 0 & 0 & 0 \\ -\beta & 0 & 0 & -\alpha & 0 & 0 & 1 & 0 & 0 \\ 0 & -\beta & 0 & 0 & -\alpha & 0 & 0 & 1 & 0 \\ 0 & 0 & -\beta & 0 & 0 & -\alpha & 0 & 0 & 1 \\ 0 & 0 & 0 & 0 & 0 & 0 & -\rho & 0 & 0 \\ 0 & 0 & 0 & 0 & 0 & 0 & 0 & -\rho & 0 \\ 0 & 0 & 0 & 0 & 0 & 0 & 0 & 0 & -\rho \end{bmatrix}$$
 and

$$T = \begin{bmatrix} 1 & 0 & 0 & 0 & 0 & 0 & 0 \\ 0 & 1 & 0 & 0 & 0 & 0 & 0 \\ 0 & 0 & 1 & 0 & 0 & 0 & 0 \\ 0 & 1 & 0 & 0 & 0 & 0 & 0 \\ 0 & 0 & 0 & 1 & 0 & 0 & 0 \\ 0 & 0 & 0 & 0 & 1 & 0 & 0 \\ 0 & 0 & 0 & 0 & 0 & 1 & 0 \\ 0 & 0 & 0 & 0 & 0 & 0 & 1 \end{bmatrix}$$

References

- [1] L. Carassale, M.M. Brunenghi, Identification of meaningful coherent structures in the wind-induced pressure on aprismatic body, J. Wind Eng. Ind. Aerodyn. (104—106) (2012) 216—226.
- [2] K. Gurley, A. Kareem, Applications of wavelet transformations in earthquake, wind and ocean engineering, Eng. Struct. 21 (1999) 149–167.
- [3] Y. Li, A. Kareem, Simulation of multivariate nonstationary random processes by fft, ASCE J. Eng. Mech. 117 (5) (1991) 1037–1058.

- [4] H. Wang, T. Wu, T. Tao, A. Li, A. Kareem, Measurements and analysis of nonstationary wind characteristics at sutong bridge in typhoon damrey, J. Wind Eng. Ind. Aerodyn. 151 (2016) 100–106.
- [5] L. Caracoglia, A stochastic model for examining along-wind loading uncertainty and intervention costs due to wind-induced damage on tall buildings, Eng. Struct. 78 (2014) 121–132.
- [6] G. Deodatis, R.C. Micaletti, Simulation of highly skewed non-gaussian stochastic processes, ASCE J. Eng. Mech. 127 (12) (2001) 1284–1295.
- [7] M. Gioffré, M. Grigoriu, M. Kasperski, E. Simiu, Wind-induced peak bending moments in low-rise building frames, J. Eng. Mech. 126 (8) (2000) 879–881.
- [8] M. Gioffré, V. Gusella, M. Grigoriu, Simulation of non-Gaussian field applied to wind pressure fluctuations, Probab. Eng. Mech. 5 (4) (2000) 339–346.
- [9] K.R. Gurley, A. Kareem, M.A. Tognarelli, Simulation of a class of non-normal random processes, Int. J. Non-Linear Mech. 31 (5) (1996) 601–617.
- [10] L.L. Yang, K. Gurley, D. Prevatt, Probabilistic modeling of wind pressure on low-rise buildings, J. Wind Eng. Ind. Aerodyn. 114 (2013) 18–26.
- [11] M.R. Leadbetter, G. Lindgren, H. Rootzén, Extremes and Related Properties of Random Sequences and Processes, Springer-Verlag, New York, 1983.
- [12] I.M. Babuška, R. Temptone, E. Zouraris, Solving elliptic boundary value problems with uncertain coefficients by the finite element method: the stochastic formulation, Comput. Methods Appl. Mech. Engrg. 194 (12–14) (2005) 1251–1294.
- [13] M. Grigoriu, Parametric models for samples of random functions, J. Comput. Phys. 297 (2015) http://dx.doi.org/10.1016/j.jcp.2015.04.053.
- [14] D.B. Hernández, Lectures on Probability and Second Order Random Fields, World Scientific, London, 1995.
- [15] J. Mercer, Functions of positive and negative type and their connection with the theory of integral equations, Phil. Trans. R. Soc. A 209 (441–458) (1909) 415–446, http://dx.doi.org/10.1098/rsta.1909.0016.
- [16] A.W. van der Vaart, Asymptotic Statistics, Cambridge University Press, New York, 1998. ISBN 978-0-521-49603-2.
- [17] P. Billingsley, Convergence of Probability Measure, first ed., Wiley, New York, 1968
- [18] W. Rudin, Real and Complex Analysis, third ed., McGraw-Hill, Inc. New York, 1987
- [19] K. Itô, M. Nisio, On the convergence of sums of independent Banach space valued random variables, Osaka J. Math. 5 (1968) 35–48.
- [20] M.B. Marcus, L.A. Shepp, Sample behavior of Gaussian processes, in: Proc. Sixth Berkeley Symp. Math. Statis. Probab. Vol. 2, Univ. of California Press, Berkeley, CA, 1971, pp. 423–442, (1971).
- [21] G. Samorodnitsky, Probability tails of Gaussian extrema, Stoch. Process. Appl. 38 (1991) 55–84.
- [22] M. Grigoriu, Existence and construction of translation models for stationary non-Gaussian processes, Probab. Eng. Mech. 24 (2009) 545–551.
- [23] F. Sadek, S. Deniz, M. Kasperski, M. Gioffré, E. Simiu, Sampling errors in the estimation of peak wind-induced internal forces in low-rise structures, J. Eng. Mech. 130 (2) (2004) 235–239.
- [24] M. Grigoriu, Stochastic Calculus. Applications in Science and Engineering, Birkhäuser, Boston, 2002.
- [25] G.P. Tolstov, Fourier Series, Dover Publications, Inc. New York, 1962.